ECOLOGICAL RESPONSES TO SEVERE FLOODING IN COASTAL ECOSYSTEMS: DETERMINING THE VEGETATION RESPONSE TO HURRICANE HARVEY WITHIN A TEXAS COASTAL SALT MARSH

Kenneth R. Hudman

Thesis Prepared for the Degree of

MASTER OF SCIENCE

UNIVERSITY OF NORTH TEXAS

August 2021

APPROVED:

Pinliang Dong, Major Professor
David Hoeinghaus, Committee Member
Feifei Pan, Committee Member
Paul Hudak, Committee Member
Jyoti Shah, Chair of the Department of Biology
Pamela Padilla, Dean of the College of Science
Victor Prybutok, Dean of the Toulouse Graduate School

Hudman, Kenneth R. *Ecological Responses to Severe Flooding in Coastal Ecosystems: Determining the Vegetation Response to Hurricane Harvey within a Texas Coastal Salt Marsh*. Master of Science (Environmental Science), August 2021, 53 pp., 18 figures, 1 appendix, references, 61 titles.

Vegetative health was measured both before and after Hurricane Harvey using remotely sensed vegetation indices on the coastal marshland surrounding Galveston Island's West Bay. Data were recorded on a monthly basis following the hurricane from September of 2005 until September of 2019 in order to document the vegetation response to this significant disturbance event. Both initial impact and recovery were found to be dependent on a variety of factors, including elevation zone, spatial proximity to the bay, the season during which recovery took place, as well as the amount of time since the hurricane. Slope was also tested as a potential variable using a LiDAR-derived slope raster, and while unable to significantly explain variations in vegetative health immediately following the hurricane, it was able to explain some degree of variability among spatially close data points. Among environmental factors, elevation zone appeared to be the most key in determining the degree of vegetation impact, suggesting that the different plant assemblages that make up different portions of the marsh react differently to the severe flooding that took place during Harvey.

ACKNOWLEDGEMENTS

I want to acknowledge my mentor Dr. Pinliang Dong for all his guidance, patience, and time that he spent with me during this long tenure as a graduate student. Also to my committee, Dr. David Hoeinghaus, Dr. Feifei Pan, and Dr. Paul Hudak for their support through this time, you all played a big role in my perseverance and getting through this process. Dr. Hoeinghaus, I remember when I first approached you with my research idea and begged you to be on my committee, that one of the things you told me before signing my committee form is at the end of it all I would hate you. While your advice and guidance has certainly given me a few sleepless nights and frantic work crunches, I'm happy to say at the end that your prediction couldn't have been more wrong, that I've appreciated every piece of advice you've given me.

I dedicate this to Carolyn S. Hudman and William T. Hudman who have been the absolute best parents a son could ask for. My father worked exceptionally hard to provide for his family and to be able to send his only son to college, and my mother pulled double duty by working hard at her job herself and never failing to be a good mom on top of it all, helping me whenever I needed it during school events and always being there when I needed her most. Both of my parents provided me with so many different lessons to guide me through life. My father taught me to be diligent in everything I do, to put all my effort into anything worthwhile, and my mother taught me compassion, empathy, and an ability to always see the best in things.

They are not alone either. I dedicate this thesis to every person who's helped me become the person I am today. I would not be here without the support I've received from friends and family and acquaintances alike. Thank you all.

TABLE OF CONTENTS

Page

LIST OF FIGURES

Page

CHAPTER 1

INTRODUCTION

1.1 Historical Overview

Coastal salt marshes have been the focus for many studies for well over a century. In 1885, Nathaniel Shaler noted the prevalence of marshlands along regions of marine coastline where wave energy was notably low, such as along the inlets of Chesapeake Bay (Shaler, 1885). This observation, and others like it, led to other scientists to investigate the specific plant communities, hydrology, and geology that led to the formation of these unique ecosystems. John W. Harshberger, in 1916, discovered that it was the combination of this low-energy environment caused by bays and barrier islands, coupled with the continuous, routine tidal regime that caused the formation of these ecosystems, creating an environment where these salt-tolerant plants can thrive (Harshberger, 1916). Other scientists focused on the specific nature of these plant communities and the dynamic between salt and fresh water. Conard and Galligar in 1929 noted how the fluctuations of sea and fresh water gave rise to a shift in the dynamic of these plant communities, recording one of the first instances of plant succession seen in this field (Conard & Galligar, 1929).

As research into the ecology of salt marshes grew, so did interest grow about large disturbances that could impact these ecosystems. In 1937, E.M. Kindle conducted one of the first studies of coastal marshland following an unnamed hurricane that severely damaged a New Jersey marshland, noting the extent of the vegetation damage that took place (Kindle, 1937). Similar studies noted how large-scale disturbance events such as hurricanes could actually introduce and erode enough sediment to meaningfully alter the shoreline in other marshlands (Brown, 1939). Other studies, such as Richard Howard's study of marsh vegetation in the

Bahamas, attempted to try to describe the role that hurricanes played in the community dynamics of coastal marshes in terms of resilience, succession, and recovery (Howard, 1950).

The rise of disturbance theory in ecology prompted a new look into the roles that hurricanes play into these ecosystems. Mark Bertness in 1987 described small scale disturbance events to be determinants of the patterns of marsh plant communities (Bertness, 1987). Zedler et al. in 1986 described large-scale disturbance events such as hurricanes to be major factors that significantly alter the plant communities of these coastal marshes, prompting rapid succession of plant species (Zedler et al. 1986). These studies, and others like them, helped define exactly what disturbances are and mean to salt marshes as an ecosystem, and how hurricanes act as these large-scale disturbances that alter the plant communities and allow for plant succession to occur.

The advent of the Landsat program and other similar space programs in the 70s became a boon for remote sensing and gave rise to the different technologies and research that is used in this particular field of study today. Prior to the advent of satellite imagery, remote sensing studies were typically conducted with aerial photographs, an example of which is Nowell and Parish's research in controlling mosquito populations in a Florida salt marsh (Nowell & Parish, 1956). Almost immediately following the advent of the Landsat program, scientists began to apply remote sensing methodologies to salt marsh ecology specifically, with Bartlett and Klemas's research in estimating *Spartina alterniflora* biomass in a Delaware salt marsh being a notable early application of satellite imagery in regards to coastal research (Bartlett & Klemas, 1980).

Beyond just the applications of remote sensing in regards to salt marsh ecosystems, ecologists have been attempting to use satellite imagery as a way to monitor vegetation health since the advent of remote sensing. Colwell's research in 1956 saw the use of aerial photography

to monitor disease among American croplands, and 1918 saw Robert Griggs study the recovery of vegetation after a volcanic event in Kodiak, Alaska (Colwell 1956, Griggs 1918). Managing to quantify data such as this however, was tricky using only remote sensing at the time. One of the earlier attempts to estimate vegetation biomass was through the use of the Transformed Vegetation Index, or the transformed ratio between infrared radiance and red radiance in satellite imagery, such as what Compton J. Tucker details in his research (Tucker, 1977). While this early research proved useful initially, the Transformed Vegetation Index proved ineffective at dealing with changes of the solar zenith angle between images. The Normalized Difference Vegetation Index (NDVI) developed a few years prior by Rouse et al. proved much more useful at accounting for this difference, although the use of NDVI did not become widespread until years later (Rouse et al. 1974).

Even before satellite imagery, concepts and methodologies of remote sensing have found their way into salt marsh ecology through a variety of avenues. Following the proliferation of LiDAR (light detection and ranging technology) during the 60s as a result of its numerous aerospace applications, scientists began to use this form of remote sensing in order to study ecological concepts, although early uses of LiDAR in this sense were confined to geologic applications. Davenport et al. in 1970 were one of the first teams of scientists to create what's known as a digital elevation model (DEM) of a British salt marsh in order to study the intertidal zone (Davenport et al. 1970). Although a variety of remote sensing methods have been demonstrated effectively in researching coastal marshes more recently (Zhou et al. 2016, Huang et al. 2014, Zhang et al. 1997), the use of multispectral imagery, coupled with the use of LiDAR point-cloud data gives additional vertical context to the overall reflectance data, and allows for

the discovery of possible relationships between vegetation reflectance and changes along an elevation gradient (Wang et al. 2009).

1.2 Background

1.2.1 Salt Marshes as an Ecosystem

Coastal salt marshes are high-value ecosystems that can be found along low-energy, estuarine coastal environments. Salt marshes act as a natural barrier against erosion and storm surge (King and Lester, 1995), and marsh vegetation plays a key role in the persistence of these coastal ecosystems (Gedan et al. 2010). This protective ability of marsh vegetation is diminished when coastal marshes are subjected to anthropogenic and natural disturbances (Laegdsgaard 2006, Schrift et al. 2008) that range in frequency (Ewanchuk and Bertness 2003, Reidenbaugh and Banta 1980) and intensity (Quintana et al. 1998, Zedler et al. 1986).

One of the many primary factors driving the ecosystem dynamics of coastal salt marshes is the relationship between this marsh vegetation and the tides. The specific community dynamics and organization of vegetation in these marshlands is driven by the constant inundation that the tides provide (Roman et al. 1984). This relationship between marsh vegetation and the tides is only able to exist due to the low-energy of the environments in which marshes are found, as wave action has been found to disrupt this relationship by acting as a sediment transport (Best et al. 2018). Thus, the very factors that govern the ecosystem dynamics in coastal salt marshes, are the ones that are the most easily disrupted during natural disturbance events such as hurricanes.

1.2.2 Hurricane Intensity

According to the New York City Panel on Climate Change (NPCC2), it is predicted that future hurricanes and storm events along the eastern coast will grow in strength and introduce

increasingly greater flooding to coastal ecosystems. A review of the characteristics of Hurricane Harvey shows an abnormally high volume of rainfall and higher storm surge (Blake and Zelinsky 2018) that contributed to a higher-than-normal amount of flooding in coastal areas. This increased flooding, among coastal salt marshes in particular, introduces substantial hydrological stress to the vegetation communities that thrive in these areas (Reed et al. 1992, Huckle et al. 2000). Common vegetation indices and other remote sensing methods have previously been used to determine hurricane response in coastal ecosystems (Streyer et al. 2013, Zhang 2020), however such previous works have been confined to large-scale studies that investigate large portions of coastline, or primarily focus on a specific vegetation species. As such, Hurricane Harvey could provide insight as to how coastal vegetation responds on a marsh-wide scale to such increased flooding and rainfall, which according to the NPCC2 could potentially increase even further.

1.2.3 Salt Marsh Zonation

As salt marsh plant communities are organized by elevational gradients in zonation patterns, the use if LiDAR lends itself well to vegetation analysis. Presently, it is assumed that mid- to high-marsh species are more vulnerable to prolonged flooding (Janousek & Mayo 2013), as longer inundation times and increased concentrations of salts and toxic substances greatly impacts productivity of plants with lower salt tolerances (Cooper 1982, Portnoy & Valiela 1997, Pennings et al. 2005), whereas low-marsh species remain more tolerant of increased salt concentrations that coincide with inundation. However, knowledge of the ranges and limitations of these vulnerabilities on a marsh-wide scale remain limited. Through LiDAR analysis and the use of vegetation indices, hurricane and flooding impacts can be estimated in specific regions of coastal salt marshes, segregated along the naturally occurring zonation in marshes as well as

factors that influence prolonged inundation such as the slope of the marsh. These zones and gradients are useful for comparing vegetation response, as the factors that influence the elevation gradients in marsh zonation such as salinity and inundation tolerance also influence vegetation response to these storm events.

1.2.4 NDVI

One of the most common vegetation indices to use when monitoring vegetation health is the Normalized Difference Vegetation Index (NDVI). As chlorophyll has a higher reflectance along the near-infrared spectrum (750 – 2500nm) comparatively with that of non-vegetative surfaces such as soil, water, and impervious surfaces such as roads and buildings, it becomes possible to estimate vegetative health by comparing this reflectance relative to the common reflectance of soil, which reflects highly in the visible red regions of the electromagnetic spectrum (600 – 750nm) (Kinyanjui, 2011). The formula used for NDVI is as follows:

$$(NIR - Red) \div (NIR + Red) \quad \text{(Eq. 1.1)}$$

where NIR is the reflectance of the near-infrared band and Red is the reflectance of the red band. Since healthy vegetation will absorb most of the visible spectrum, in this instance the red band, and reflect a large portion of the near-infrared band, this calculation measures the normalized difference between those two bands and returns a value between -1 and 1. Values closer to 1 indicate that the given area has a high concentration of chlorophyll, which is indicative of healthy vegetation. Unhealthy vegetation, or bare soil, will show the opposite. Unhealthy vegetation absorbs less of the visible spectrum and reflects less of the near-infrared band, which reduces the value of the index closer to -1.

Impacts of disturbance events on vegetation have previously been studied with the use of vegetation indices and remotely sensed imagery (Rodgers et al. 2009), with the Normalized

Difference Vegetation Index (NDVI) being the most common. NDVI uses multispectral imagery to determine the difference between the near-infrared and visible reflectance of vegetation cover to estimate the density of green vegetation in a given area (Weier and Herring, 2000).

1.2.5 Limitations of Remote Sensing

One of the weaknesses of these remote sensing methods described is that, for each method, only one aspect of the target area is described, without much chance for context-derived observations to occur like *in-situ* collection methods would allow. For example, the use of satellite imagery in reality simply measures the absorption and reflection of light across pre-determined bands in the area of a defined spatial resolution. Satellite imagery on its own offers no information on the plant species that make up a given area, nor does it provide any sort of vertical context to the reflectance data projected. However, by using multiple types of remote data collection, it is possible to gain some of the context that is lost on collection.

1.2.6 Potential of Slope as a Variable

While not explicitly researched, it is possible that the slope of the marsh could be a key variable in determining the vegetation response to a hurricane as a severe disturbance event. Hurricane Harvey, specifically, has been previously determined a significant hydrologic stress event for many plant communities (Sebastian et al. 2019). Additionally, research into previous flooding events highlights the role that topography and slope play into the severity of flooding, although no research of this nature has yet to be conducted in salt marsh ecosystems (Langbein 1947, Lyu et al. 2016).

1.2.7 Purpose of Current Research

The purpose of this study is to investigate the effects that slope and other environmental

factors have on the initial impacts and recovery of vegetation after an abnormally strong major hurricane event. By analyzing which portions of the marsh suffered the most damage during this extreme hydrologic stress event, this study offers further context to previous studies focusing on the role hurricanes play in salt marsh ecology. Furthermore, an analysis of the key roles that these factors play in the impact mitigation and recovery of vegetation following a major disturbance event such as Hurricane Harvey and future hurricanes like Harvey could be used to aid future conservation efforts to protect these important ecosystems.

Although the use of vegetation indices has been previously used to identify severe storm impacts on coastal communities (Steyer et al. 2013), increased hurricane frequencies and severity suggests that a closer look be taken into the specific role that prolonged flooding from these events could play into salt marsh persistence (NPCC2 2013). Salt marshes are heavily influenced by tidal regimes and, to a lesser extent, salinity (Kunza and Pennings, 2008). This forces the plant communities to organize into a series of elevational gradients and zonation patterns where less competitive, but resilient species occupy the low marsh zone, while highly competitive, but less resilient species occupy the high marsh zone (Chapman 1974, Engels & Jensen 2009). As sea-level rise already threatens mid- and high-marsh species that are less tolerant to sustained flooding, a sudden-intense storm event could trigger a mass die-off that would speed up this segregation process (Touchette et al. 2019, Conner at al. 1989). As a key component of coastal ecosystems, identifying exactly how this prolonged flooding affects marsh vegetation, and the responses thereof, is critical in continuing their management and conservation.

1.3 Hypotheses and Major Objectives

1.3.1 Hypotheses

1: LiDAR-derived slope affects the initial vegetation response following Hurricane

Harvey and directs the vegetation response well into recovery.

2: The areas corresponding to the high-marsh zone will show a greater change in NDVI following the hurricane than areas corresponding to the low-marsh zone on a marsh-wide scale.

1.3.2 Major Objectives

This study attempts to answer two main questions in regards to vegetation health following Hurricane Harvey. Firstly, which portions of the study area suffered the most vegetation damage due to Hurricane Harvey, and which environmental factors contributed the most to this damage? Secondly, is there a difference in recovery among these different portions in the months following the hurricane event?

CHAPTER 2

STUDY AREA AND DATA

2.1 Study Area

The specified area for this study was determined based on three factors: proximity to the travel path of Hurricane Harvey, presence of clearly-defined marsh zones, and availability of third-party data for analysis. In accordance with these criteria, this study is primarily focused on the salt marshes in the West End of Galveston Bay. In order to provide an adequate baseline for the analysis of this study, multispectral and LiDAR data were collected from before the 2017 hurricane from third-party sources on a historical basis using monthly data from 13 years prior to the hurricane. In addition to just the historical data, imagery was collected from the study area on a monthly basis following the hurricane for two years following the event. This was determined due to data availability for the study area as, at the time of collection, data was not yet available for 2020.

Figure 2.1: Flight path of Hurricane Harvey. Study area is outlined by the red square near Galveston.

Though not in the direct flight path, Galveston and its surrounding marshes suffered over 20" of rainfall within a 5-day period as well as storm surges over 4'.

The images chosen for this study also in effect shape the outer extent of the study area. ArcMap software from ESRI has capabilities that allow the user to "clip" an image by the spatial extent of a polygon or other image, leaving the user with a copy of the original image that is confined to the spatial extent of whatever polygon or image they used to clip the original by. Since the digital tiles generated from the satellite images and LiDAR point cloud data do not all share the same extent, the true boundaries of the study area were created by clipping each image by its temporal neighbor in ArcMap. This creates a digital extent that shrinks whenever an image is introduced that has a decreased area relative to that of the spatial extent of the previous image. In essence, the spatial extent of the study area was created by combining all the shared areas of the satellite images together.

2.2 Data

2.2.1 Satellite Imagery

Landsat 7 TM, Landsat 8 TM, Landsat 5 TM1, and Sentinel-2B images were used in this study to determine changes in NDVI values both pre- and post-Hurricane Harvey. Landsat 8, 7, and 5 images were chosen due to their availability and low cost, despite having a more moderate spatial resolution of 30m. Regardless of image origin, the primary criteria for selecting images in this study was the requirement that the study area in the image be cloud-free or mostly cloud-free, as the presence of clouds results in errors that affect an accurate index calculation. For Landsat 5, 7, and 8 images, the difference in image source is minimal, as both satellites deliver results using the same geographic coordinate system and spatial resolution (meaning the pixels from different images line up neatly with one another). Sentinel-2B images however, needed to be resampled to account for these differences in spatial resolution (10m) and coordinate system. For months with multiple image sources available with low cloud cover, those images that were

sampled closer to the beginning of the month were chosen, in order to minimize the temporal variability in the time periods between each image.

2.2.2 LiDAR

LiDAR data for this study was acquired from the Texas Natural Resources Information System (TNRIS) as part of their collaboration with Fugro USA Land. Data for this collaboration took place between January 13 and March 22, 2018, with quality control and data verification performed by AECOM. This 2018 LiDAR data was chosen over other available options due to its proximity temporally to Hurricane Harvey, which offers the best estimation to the topographical conditions immediately following the hurricane. Cahoon et al. (1995) and Baumann et al. (1984) found that marsh topography can be severely altered after hurricane events due to large washes of sediment being deposited via storm surge. Cahoon et al. specifically noted that this change in topography can alter inundation times which, in the context of this study, has the potential to produce errors in our results if this change in topography is not taken into account. To account for this potential error, the available 2018 LiDAR dataset described was used over a dataset that was collected before the hurricane, such as the Texas Parks and Wildlife's 2015 LiDAR dataset.

2.3 Pixel Classification

2.3.1 Marsh Groups

In order to distinguish between the various geographic characteristics of the study area that may be difficult to quantify, it was necessary to group like areas of the marshland into specified regions as shown in Fig. 2.2. For example, it has been shown previously that the bay side of a barrier island experiences decreased wave action that results in a much different topographical profile than the inland shore (Bird & Ranwell, 1964). Thus, all marshland of this

type was grouped into Group 1. Similarly, the marshland in Group 3 likely experiences greater wave action on a regular basis and would have the topographical profile to match. Group 4 and Group 2 are both groups of marshland that are positioned more inland than Groups 1 and 3, and would potentially be insulated from storm surge, although Group 2 may experience less of this insulation, as it lies in closer proximity to Galveston Bay than Group 4.

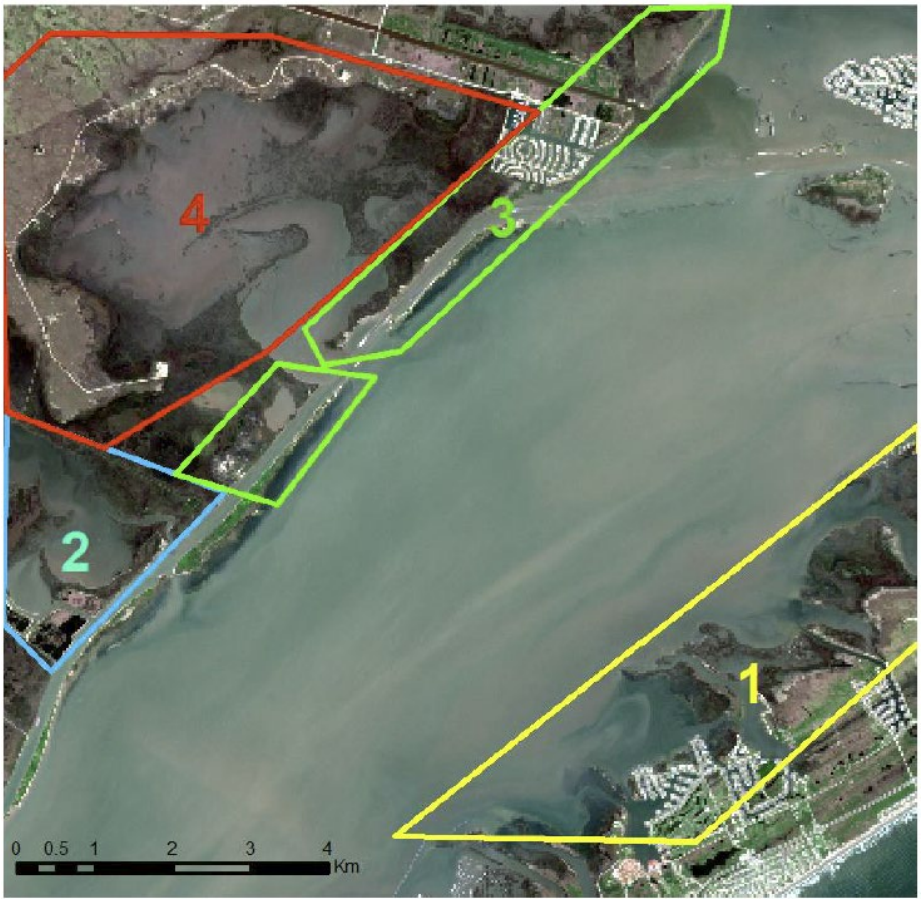

Figure 2.2: Study area and marsh groups as viewable in Google Earth.

Shown is a true color image of Chocolate Bayou and the West End of Galveston Bay, TX

In order to quantify contextual information such as this, it was important to establish these groups as a sort of classification variable. As these groups are comprised of abstract classifications of environmental factors that are difficult to quantify, the exact spatial extent and delineation of these groups is less important than the justification of why these groups are

chosen. Additionally, it benefits these arbitrary group classifications to be larger than initially suspected, as the practical application of these groups is to assign a sort of classification to specific areas of the data that is described in the next section.

2.3.2 Elevation Zone

To delineate between different elevation zones of the marsh, as well as to distinguish between salt-marsh pixels and freshwater/non-marsh pixels in the images, a shapefile was downloaded from the National Wetlands Inventory (NWI) that contains information on the extent and characteristics of the marshland that were investigated in this study. As this NWI shapefile contains a myriad of classifications that have uses beyond this study, it was necessary to group all the classifications of a single elevation zone into a single shapefile.

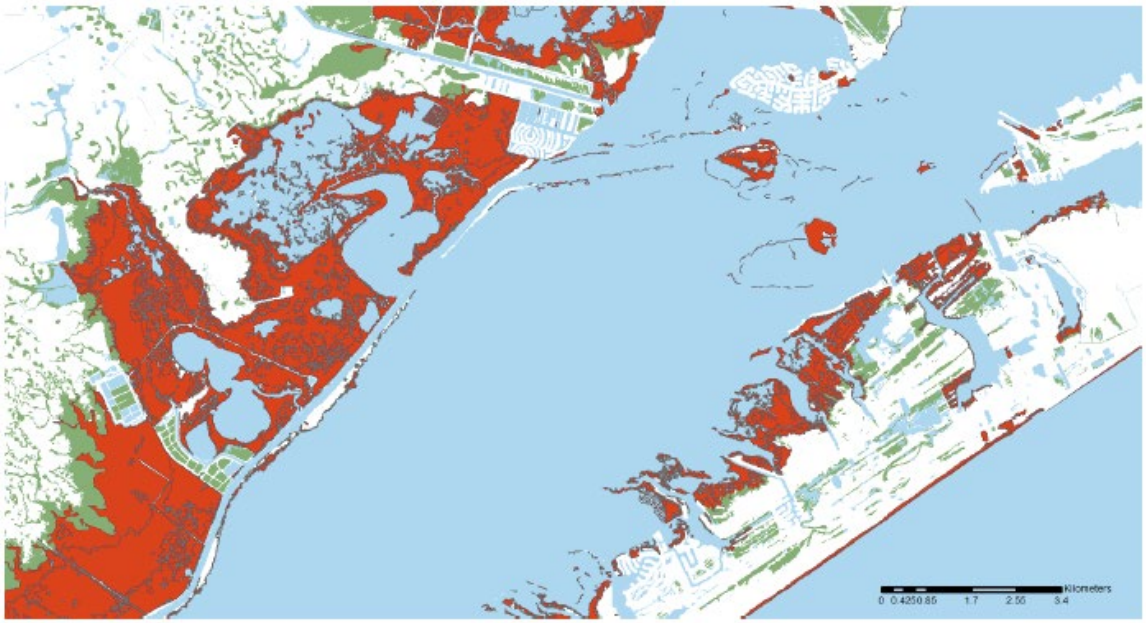

Figure 2.3: Shapefile of recorded wetlands in the study area as viewable in ArcMap.

Red areas correspond with estuarine and marine wetlands while green areas correspond with freshwater emergent wetlands. Derived from the National Wetlands Inventory.

For the purposes of this study, all wetland classifications that are described as having a "regularly flooded" tidal regime are used to describe the low marsh zone, whereas wetland

classifications that are described as “irregularly flooded” are used to describe the high marsh zone. The “subtidal” and “irregularly exposed" classifications were not used for this study, as the regular presence of water in satellite imagery has the ability to disrupt NDVI calculations. Furthermore, an additional shapefile was developed in order to distinguish between the nominal marsh areas that were previously described, using the spatial extents seen in Fig. 2.2.

CHAPTER 3

METHODS

3.1 Image Pre-processing

In order to accurately use the satellite imagery, preliminary processing had to be made on each image to ensure that whatever band information was extracted reflects the properties of the ground below, and is not obscured by clouds that slipped through the initial data selection process. To do this, a cloud mask was applied over each Landsat image in the study. ArcPy (the ArcGIS python library) contains functions that allow the software to identify individual pixels that are likely to be clouds, and mask them from further data analysis by assigning them a null value. For quality assurance of the study data, this process was done on each satellite image in the study. In addition to the cloud mask, each Landsat 5 image needed to be transformed so as to accurately depict reflectance data rather than 8-bit digital number. The process for completing this transformation can be found in Vogelmann et al. (2001). As Sentinel-2 images are naturally converted to reflectance in the 1C processing level before the cloud and atmosphere mask is applied, no transformations were needed to extract NDVI values from Sentinel-2 images. Additionally, each image in the study had to be clipped down to ensure the same spatial extent and geographic coordinates applied to each image in the study. Since misaligned pixels could potentially obscure the results of the study, this step was vital in ensuring that each pixel of the satellite imagery would align along the same spatial extent. It was during this step that resampling was performed for Sentinel-2 images, creating a change in spatial resolution that would allow for comparisons between Sentinel-2 and LANDSAT images to occur. Resampling in this step was performed using the ArcMap resampling functionality using the nearest neighbor resampling method. Using this method, each new pixel in the Sentinel-2 image raster was

assigned a value equal to that of the old coordinate pixel nearest to that of the new pixel. This method allows for the most efficient resampling method in regards to computing time while also achieving a sufficiently accurate raster in regards to preserving the values of the old raster in a spatial context (Parker et al. 1983).

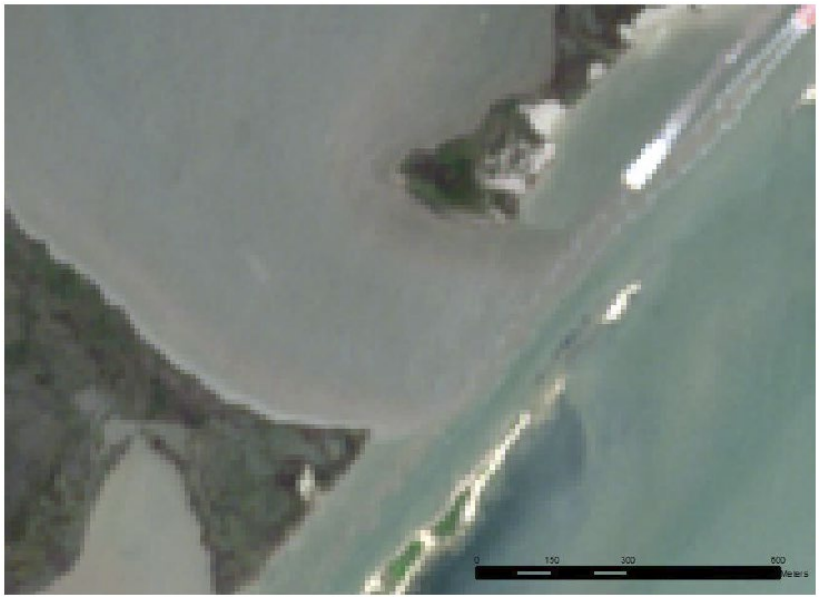

Figure 3.1: Sentinel-2 satellite imagery before resampling, with a spatial resolution of 10 meters per pixel

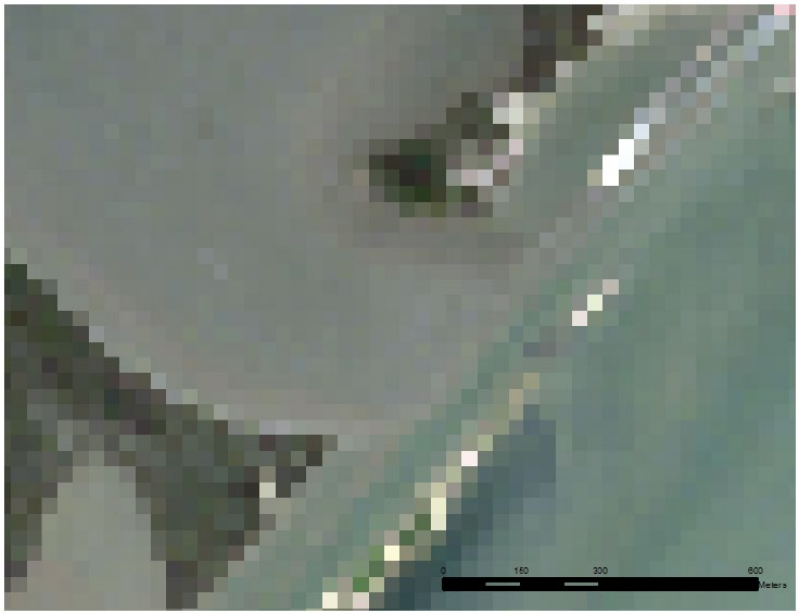

Figure 3.2: Sentinel-2 satellite imagery after resampling. Spatial resolution has been decreased to 30 meters per pixel to allow for comparisons with LANDSAT imagery

3.2 NDVI Calculations

Similar to Steyer et al. (2013), commonly-used vegetation indices were used to analyze vegetation response to Hurricane Harvey. For this study, NDVI was used, as NDVI is useful at monitoring overall chlorophyll concentration, which is a useful metric for estimating primary productivity of an ecosystem. In order to determine NDVI for this study, the calculation for NDVI had to be performed at the base level for each of the monthly images in this study. The mosaic function in ArcMap allows for this calculation to be performed for each pixel in the image. After extracting the values for each pixel from the near infrared and red band, the NDVI calculation was applied across the entire image. As NDVI is a normalized index, this calculation would assign each pixel in the satellite image a value between 1 and -1 (Except for those pixels removed via the cloud mask and transformations described earlier).

Figure 3.3: Sample NDVI raster from the study area. Data is derived from the September 2017 imagery. Lighter areas correspond to an NDVI closer to 1, while darker areas correspond to an NDVI closer to -1.

3.3 Creation of Slope Raster

For the LiDAR processing, the data needed to first be converted from a point cloud format to a typical raster. As LiDAR point cloud data is essentially the raw return data that is derived from the initial LiDAR flyovers, this makes point cloud data an ideal starting point for many LiDAR applications, including its use in this study. To begin processing, it was first necessary to determine exactly which returns were ground returns and which were vegetation, as each "point" in a LiDAR point cloud contains multiple returns from the same physical space. Since the strength of these different types of returns is inequal however, it was possible to determine ground returns using the return classification abilities in ArcMap. After discarding all non-ground returns, a more traditional raster was then created in ArcMap by sampling all of those returns into 30m pixels that had the same resolution and coordinate system as the satellite imagery. This was achieved through the same nearest neighbor interpolation method that was described previously in this chapter, although nearest neighbor interpolation with LiDAR point clouds usually involves an extra step. Since LiDAR point cloud data formats are not inherently gridded into a matrix like raster datasets are, a grid needed to first be specified to fit over the LiDAR point cloud. This is actually a relatively simple process, as this study already uses a grid format that can be used for this LiDAR dataset. By applying a grid with the same spatial resolution and coordinate system as the satellite imagery in this study, the LiDAR point cloud can easily be sampled into a format similar to the rest of our data. Additionally, any void spaces in the LiDAR dataset (which can sometimes happen due to errors in gridding, though was not expected with a grid size of 30m) were assigned a value equal to the linear relationship between the neighboring points.

Since LiDAR data often comes in smaller tiles to allow for faster data processing, it was

necessary to merge these smaller rasters together to obtain a larger raster that covered the entire study area. This raster, called a digital terrain model (DTM), acts as a topographic profile of the study area. Of this LiDAR raster, a slope raster was created in ArcMap by using the values of each cell and its neighbors to determine the changes in distance and verticality of each cell, giving a raster where each cell has a slope value between itself and its neighboring cells.

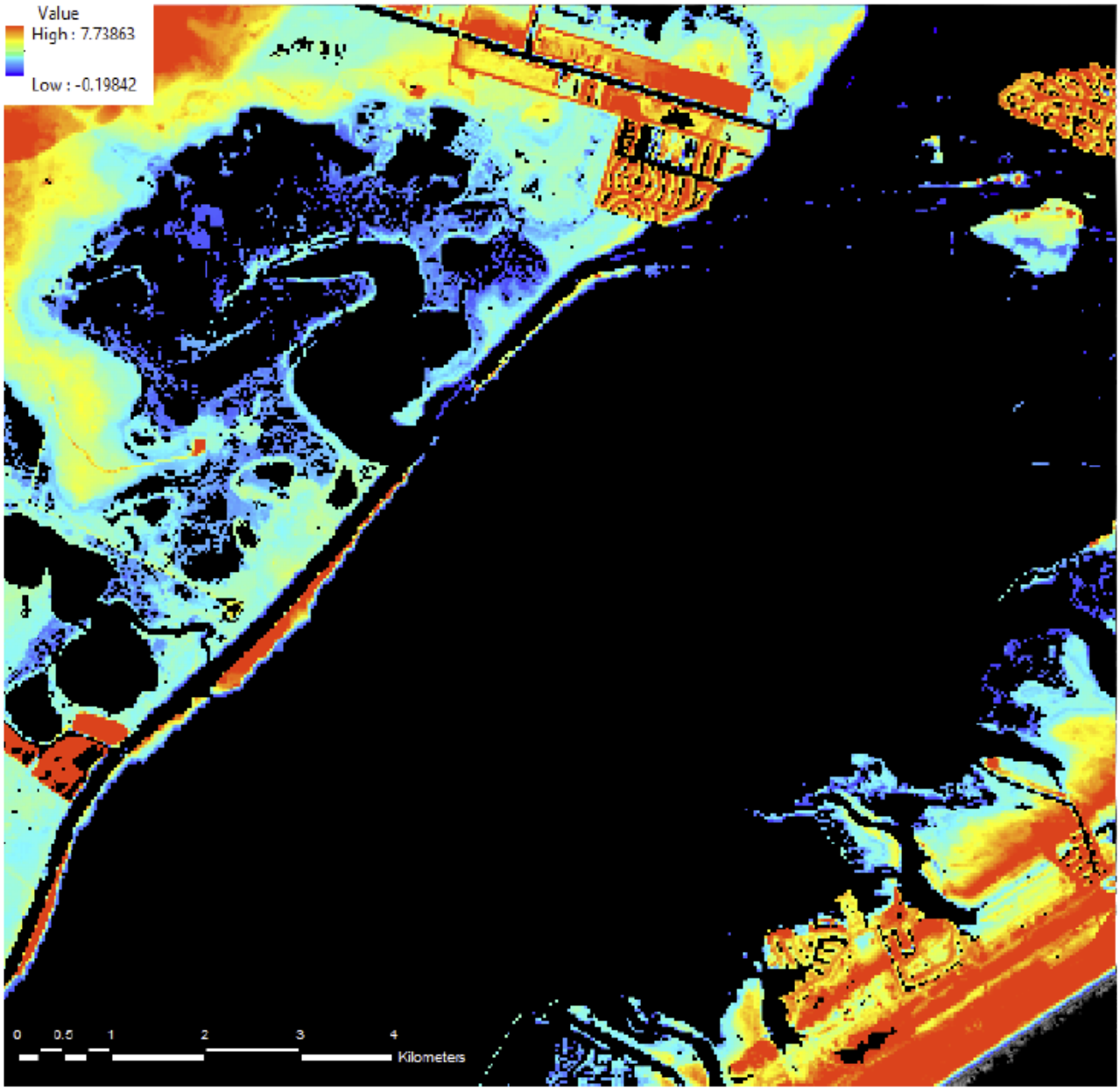

Figure 3.4: Digital Terrain Model (DTM) of the study area. Red areas represent pixels with a higher elevation, while blue areas represent pixels closer to sea level.

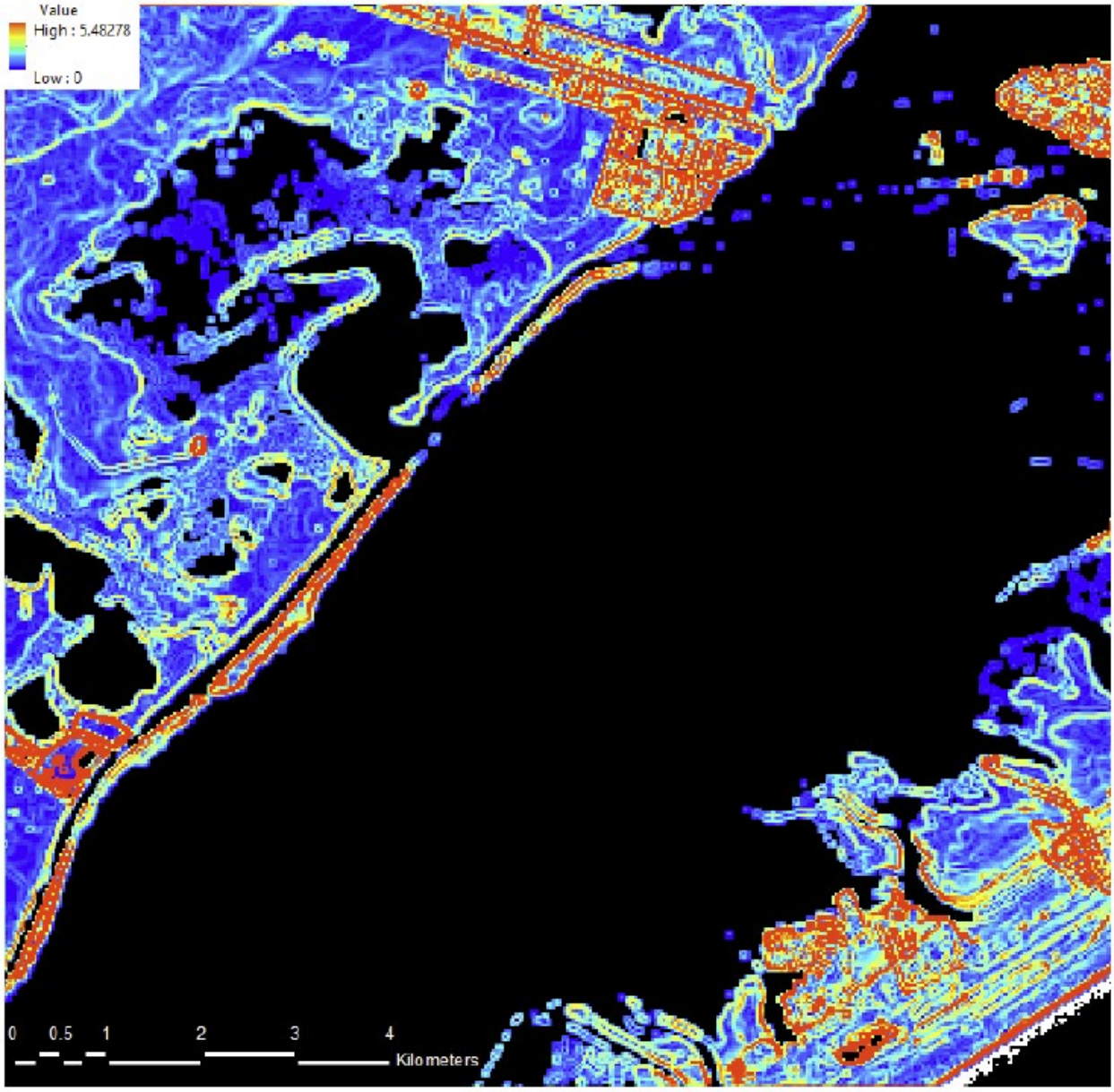

Figure 3.5: Slope raster of Study Area. Blue pixels represent patches of flatter land with a slope closer to 0, while Red pixels represent patches of steeper land with a higher slope

3.4 Shapefile Clipping and Data Extraction

Each of the shapefiles described in the previous section were used to help define the nominal variables for this study. These two shapefiles, when taken together and clipped, allow for each image to be broken down into the pixels that make up each individual marsh "portion" that exists in this study (high marsh zone and low marsh zone for each of the four previously

described areas, for a total of 8 portions of marshland). For each of these "portions" of marshland, approximately 100 pixels were randomly selected out of the available area to serve as the basis for the statistical analysis of this study. The selection process for this random generation was performed in ArcMap, using a minimum distance of 60m between the randomized points to prevent multiple points occupying the same pixel of satellite imagery. Once generated, these random points (917 in total) were compared to each satellite image in the study area, to remove points that were generated in primarily submerged portions of the marshland (as the NDVI calculation from submerged pixels would yield errors in our results). Once primarily submerged points were removed, the remaining points (845) were given NDVI values based on the underlying pixels from the available imagery. As multiple images can be layered atop one another spatially, it is possible for one point to contain multiple values from each underlying layer. These NDVI values from each image in the study and slope value were extracted to each of the randomized points generated, allowing each randomly generated point to contain a specified NDVI value for each month of data both before and after Hurricane Harvey, as well as a slope value from the slope raster that was generated. Latitude and longitude coordinates were additionally added to the list of values associated with each of the randomly generated points, in order to give them an X and Y value associated with the study area. Additionally, the nominal variables in this study, elevation zone and area ID, were added to this table of values based on where the randomly generated point originated spatially. From there, the data was analyzed using a variety of mixed modeling methods described in the next section.

CHAPTER 4

RESULTS AND DISCUSSION

4.1 Transformation

The fundamental assumption of this study was that the effects of Hurricane Harvey would impact the vegetation to such a degree that a change in the concentration of chlorophyll could be detected from remotely-sensed imagery. This was recorded not through a raw NDVI change, as historically month-to-month NDVI changes can be quite chaotic, but instead was recorded by a transformation in which the NDVI value for one month was compared to the NDVI values for similar months in different years of the study. As this study used images from a period of 15 years, including the year of the hurricane, this meant that each month had approximately 15 similar months with which to compare NDVI values. Therefore, a transformation was applied to the raw NDVI values in order to show this change in reference to what could be considered "normal" for that specific month. The formula for this transformation is given by:

$$DN_{jik} = NDVI_{jik} - med(NDVI_{ji}) \quad \text{(Eq. 4.1)}$$

where DN_{jik} is the transformed difference between the NDVI value for month *j* and year *k* at point *i*, and the median NDVI value for month *j* and pixel *i* across all other years. For this study, we chose to include negatives as part of this transformation, as it creates directionality of these NDVI changes that are useful when analyzing hurricane impacts.

4.2 Early Data Exploration

Examination of the data shows a clear decrease in the NDVI from August 2017 to September 2017 immediately following the hurricane (Figs. 4.1 and 4.2), with a maximum decrease of .72 among individual points and .17 on average.

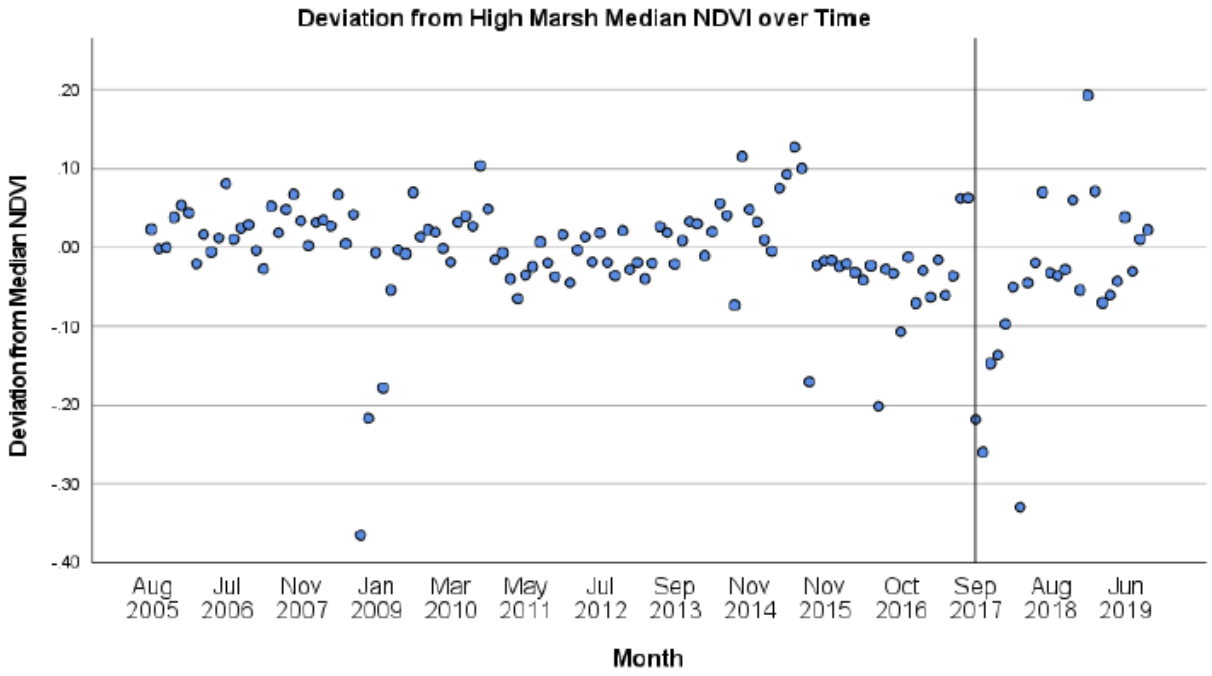

Figure 4.1: Time series of the deviation from the monthly median NDVI across the entire study period for the high marsh zone. The vertical bar represents when Hurricane Harvey took place.

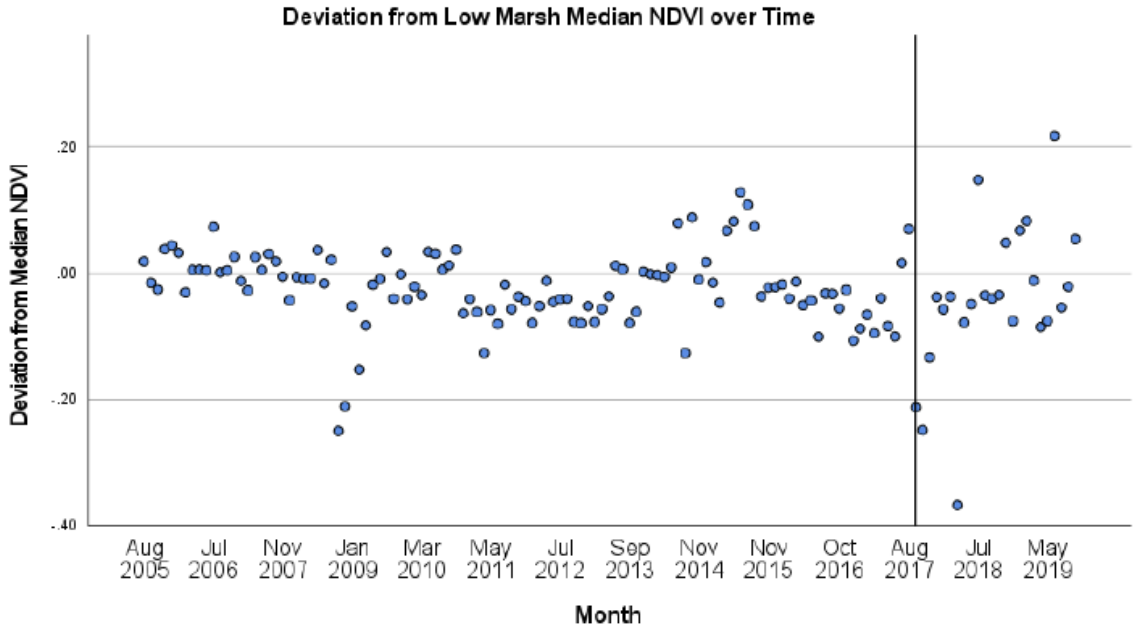

Figure 4.2: Time series of the deviation from the monthly median NDVI across the entire study period for the low marsh zone. The vertical bar represents when Hurricane Harvey took place.

In October of the same year, this decrease persisted, with a maximum decrease of .6 among individual points and an average decrease of .25. There appeared to be a second, delayed

dip in NDVI in April of the following year as well, averaging approximately to a decrease of .34 among all points. Only in the summer of 2018 did the trend reverse and an increase in NDVI appear for both marsh zones, averaging approximately .105 across all points during the month of July. This apparent bloom showed up again in early 2019, showing an increase in NDVI across both the high and the low marsh by .19 and .06 respectively before finally returning to some normalcy in March of 2019.

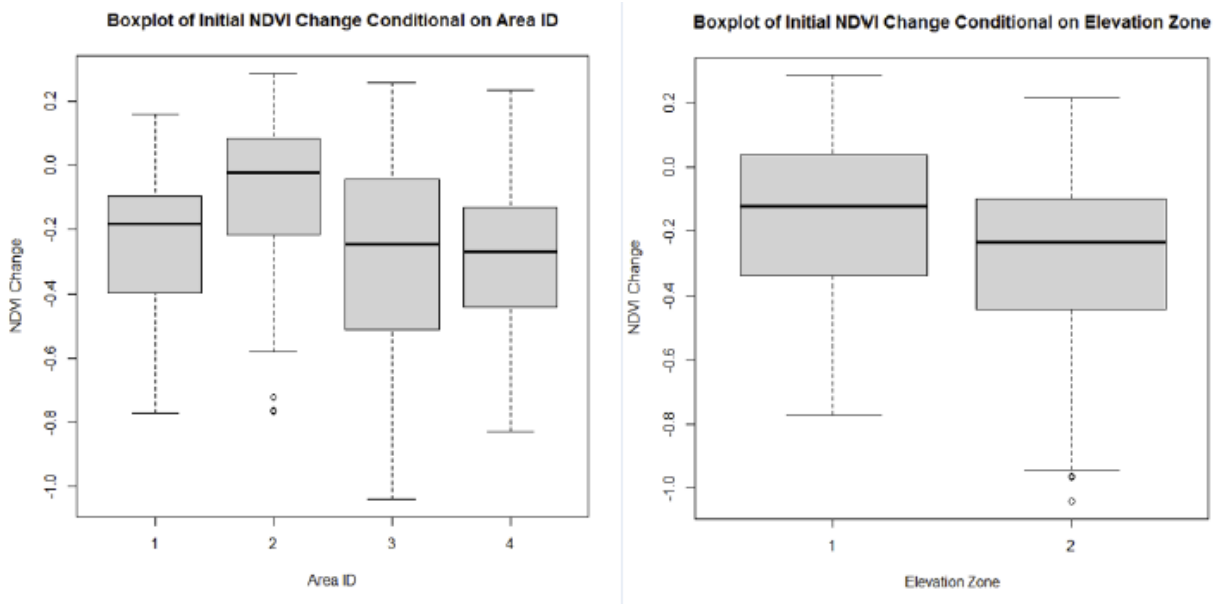

Figure 4.3: Boxplots of significant spatial variables. Elevation Zones 1 and 2 needed to be converted to numerical form temporarily and correspond with Low and High marsh zones respectively.

Grouping this initial change by the nominal variables in our study yielded interesting results. Although not independently sampled, a comparison of means between the high marsh zone and low marsh zone revealed that the initial change in the high marsh zone is almost double that of the low marsh zone (low marsh: -.112, high marsh: -.218), although the high marsh zone appeared more prone to outliers. An early analysis of the group IDs yielded similarly interesting results. Area 2 appeared to suffer the least initial vegetation damage, with a mean NDVI decrease only a fraction of that of other areas (Area 1: -.193, Area 2: -.011, Area 3: -.202, Area

4: -.231). Much like the high marsh zone previously discussed however, it appears that Area 2 was more prone to outliers than that of other areas. A comparison of the variances of the affected areas also revealed interesting results, as Area 3 appeared to have the highest variance across the four areas (Area 1: .043, Area 2: .036, Area 3: .084, Area 4: .051), while the least affected area (Area 2), had the lowest variance among the four areas of the study.

As a first analysis, we applied a multiple regression model using slope, elevation zone, designated marsh area, season, and time since the hurricane as explanatory variables and the transformed NDVI change as a response variable. This approach however, ran into issues when attempting to nest certain variables such as time or slope on a per-point basis. Additionally, violations of spatial and temporal independence needed to be addressed that a simple multiple regression couldn't solve. As it was unclear with this preliminary regression whether temporally or spatially close data points were correlated, it suggested that a more advanced modeling method needed to be used.

4.3 Spatial Independence

4.3.1 Initial Model

To solve the issue of spatial independence, and to address the first question that this study attempts to answer, it was necessary to narrow our focus temporarily to the first month after the hurricane, September 2017, in order to understand which portions of the marsh were affected the most by the initial impact of this disturbance event. For the initial data exploration, we applied a linear regression model using all the possible explanatory variables that were in our dataset. The initial regression model is given by:

$$DN_i = a + factor(Elevation\ Zone_i) + factor(Area\ ID_i) + \beta_1 R_i + \beta_2 X_i + \beta_3 Y_i + \varepsilon_i \quad \text{(Eq. 4.2)}$$

where DN_i is the deviation from median NDVI for September 2017 for point i, a is an intercept, $factor$ is a factoring function so our nominal variables can be included in the regression, R_i is the slope derived from the LiDAR slope raster, and X and Y are the latitude and longitude coordinates. ε_i is independently, normally distributed noise with a mean of 0 and variance σ^2. Fitted values based on the initial regression are shown in Fig. 4.1. Comparing the coefficients for all explanatory variables showed there was no statistically significant latitudinal, longitudinal, or slope effect on the initial change in NDVI (X: p = .739, Y: p = .981, slope: p = .131), nor on later temporal periods when this regression was replicated (X: p = .998, Y: p = .568. slope: p = .191 for the month of October). Consequently, both the functions for area ID and elevation zone proved highly significant (Area ID: $p < 2e^{-16}$, Elevation zone: $p < 2e^{-16}$) and can be visualized in Fig. 4.2, though this relationship weakened when this regression was performed on a later month (Area ID: p = .0012, Elevation Zone: p = .0026). Additionally, this regression model suffered from spatial heterogeneity, shown in variogram Fig. 4.4, which indicated that a more complex model was necessary in order to include a spatial correlation structure that could solve this issue. The following model chosen was a generalized least squares (GLS) that was fit for this spatial data:

$$DN_i = a + factor(Elevation\ Zone_i)\beta_1 + factor(Area\ ID_i)\beta_2 + \varepsilon_i$$

$$E[\varepsilon] = 0 \quad Var[\varepsilon] = \sigma^2 V \qquad \text{(Eq. 4.3)}$$

where DN_i is the deviation from the median NDVI in September 2017 for point i, a is an intercept, $factor$ is a factoring function so our nominal variables can be included in the regression with slope β. ε_i is independently, normally distributed noise with a mean of 0 and variance σ^2, where V is a known n x n matrix.

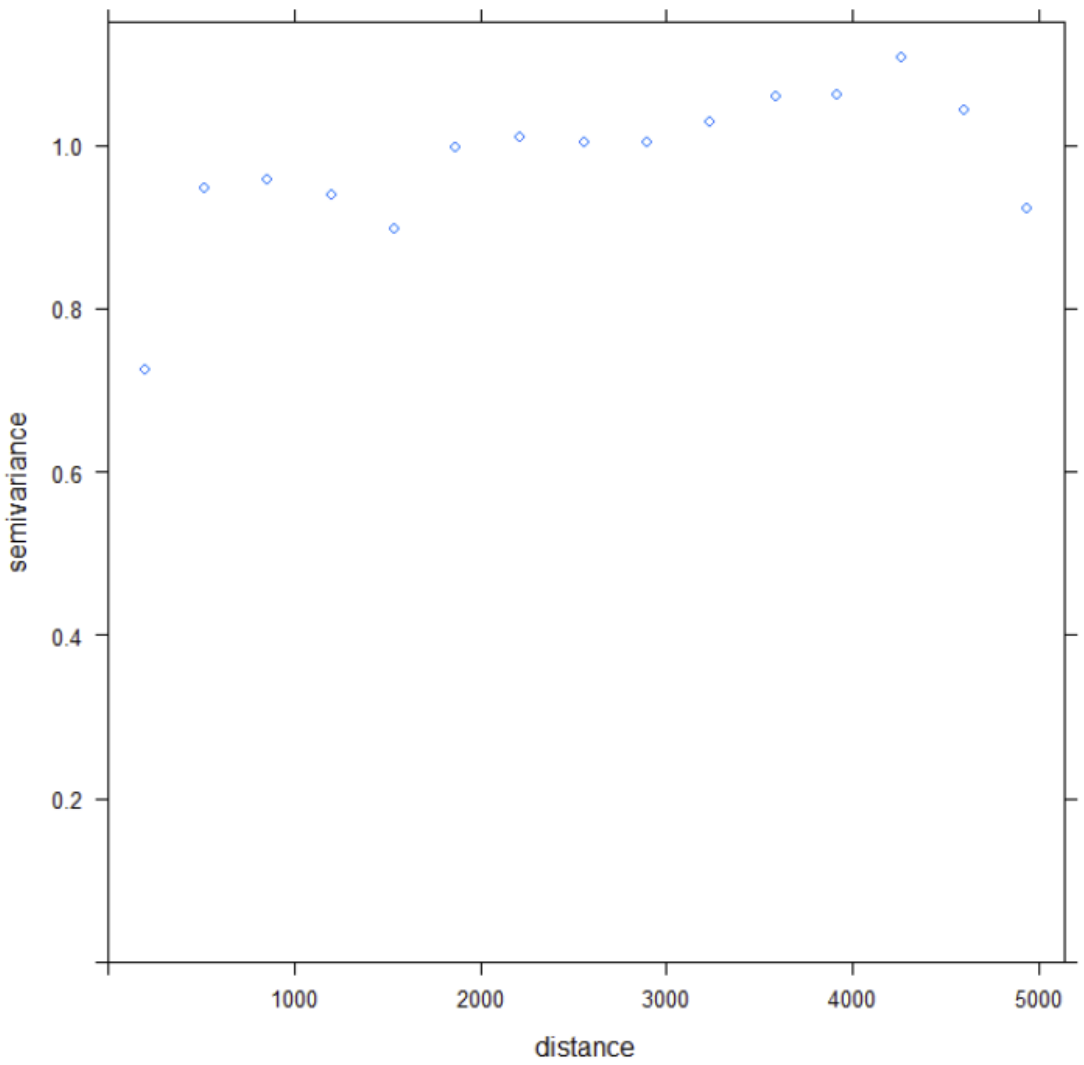

Figure 4.4: Variogram of the initial regression model. Note the correlation trend in regards to the distance between points.

4.3.2 Correlation Structures

To explore potential correlation structures for this model, six different types of correlation structures (exponential, Gaussian, linear, rational, spherical, and no correlation) were fitted onto the above model and compared using both the Akaike Information Criterion (AIC) and an analysis of variance (ANOVA) on the residuals. The results of this test determined that adding a gaussian correlation structure yielded a significantly better model (AIC = 31.715, $p < .001$), while also greatly reducing heterogeneity in the residuals (Fig. 4.5).

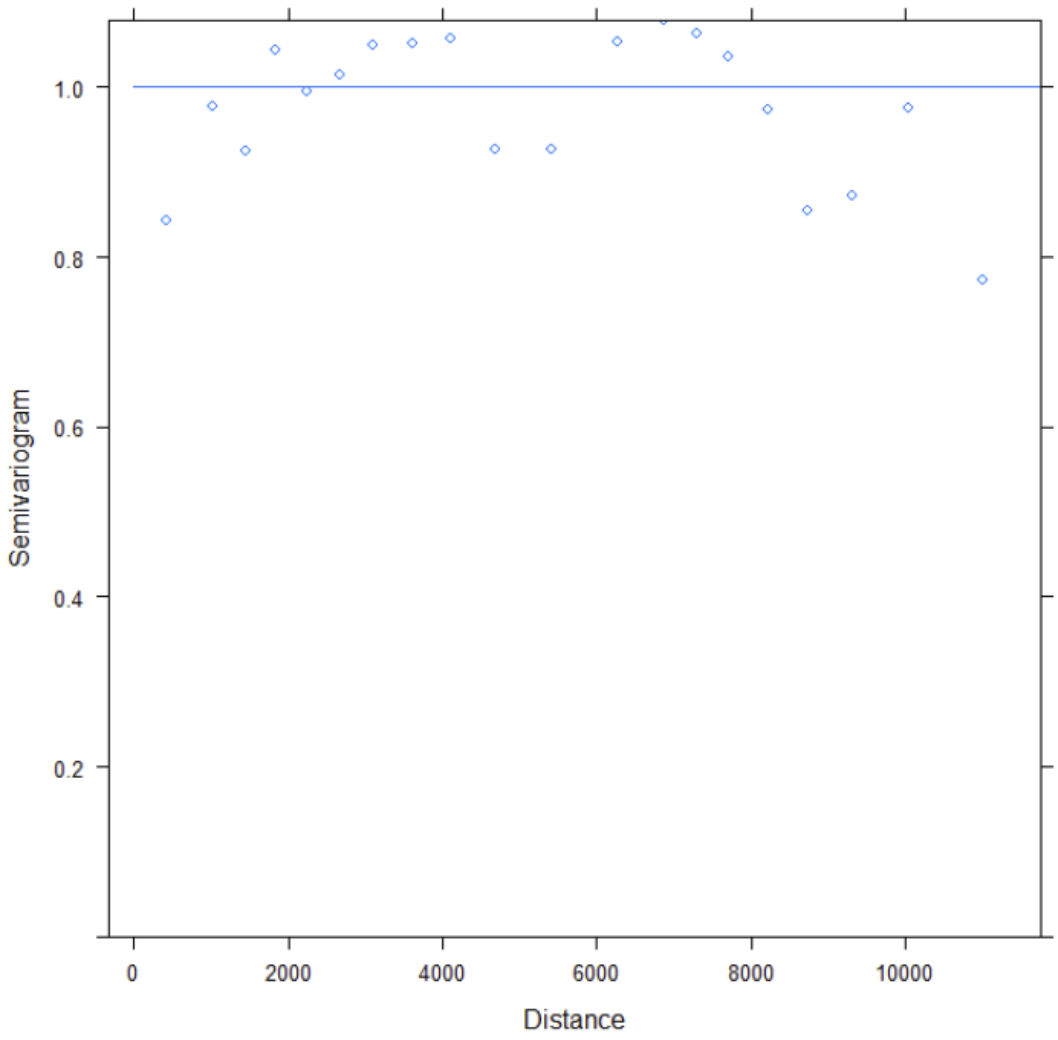

Figure 4.5: Variogram of the improved model with correlation structure. Blue line represents a smoothing spline that was applied to show trends in semivariance

4.4 Temporal Independence

4.4.1 Initial Model

To solve the issue of temporal independence in any potential model that we make, a slightly different approach needed to be taken with the data. Nesting ~840 data points for each month of data runs the risk of computational issues in data analysis, and trying to fit a complex regression model to the data becomes difficult when working with a model with such a high number of degrees of freedom. Therefore, it was determined that spatial structures such as slope

and coordinate data needed to be dropped in order to combine all the points of a single marsh "portion" to use as an average for each month. As these spatial variables were previously determined to not be statistically significant, it was not anticipated that this grouping would drastically alter the model, and such a method allowed us to solve the nesting conundrum presented above as well as cut down on the degrees of freedom that would hinder the fit of a complex model. Early data exploration of a simple multiple regression model indicated that while variables such as time since the hurricane, elevation zone, area ID, and season are all statistically significant ($p < .05$), issues of homogeneity are clearly established (Fig. 4.6), and a more advanced modeling method that can account for these sorts of correlation structures needed to be implemented.

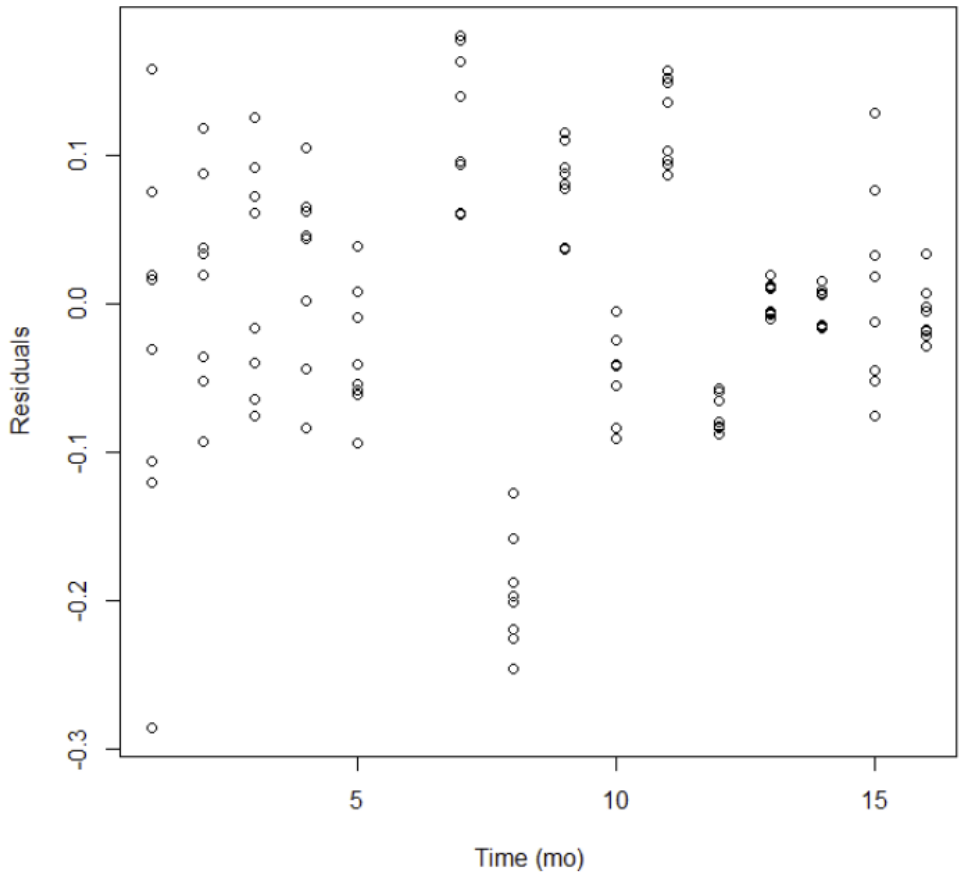

Figure 4.6: Residuals of initial smoothing model plotted over time. Not that heterogeneity occurs when plotting the residuals along a temporal scale.

4.4.2 GAMM

To implement a correlation structure into a dataset like this one that is nested by elevation zone and area ID, a generalized additive mixed model (GAMM) was used in order to implement a random effect for each observation. Additionally, by using a GAMM, it was possible to fit a different smoothing function for each geographic "portion" of the study area. The formula given by this model is:

$$\begin{aligned} 〚DN〛\_jh &= a + factor(\ 〚Elevation\ Zone〛\_jh\ ) + factor(\ 〚Area\ ID〛\_jh\ ) \\ &\quad + f\_k\ (T\_j\ ) + factor(S\_j\ ) + \varepsilon\_jh \\ var(\varepsilon_{jh}) &= \ {\sigma_k}^2 \end{aligned} \qquad \text{(Eq. 4.4)}$$

where DN_i is the deviation from median NDVI during month *j* for observation h, a is an intercept, $factor$ is a factoring function so our nominal variables can be included in the model. f is a smoothing function that is distinguished by elevation zone and area ID. k is an index attached to the smoothing function and multiple variances that allows for each combination of elevation zone and Area ID to have its own time-NDVI profile. T is the time in months since the hurricane, Elevation Zone and Area ID are our geographical nominal variables, and S is the season. ε_i is independently, normally distributed noise with a mean of 0 and variance σ_h^2, where each nested observation is allowed to have its own variance. In this case, the nested variables are elevation zone and area ID.

Comparing the deviances of this model to others with differing correlation structures showed this model to be the most optimal (AIC = -142, $p < .001$). Comparing the variances of the fitted curves of this model showed all explanatory variables to be statistically significant, though seasonality in particular was much more statistically significant than any other parametric term (Seasonality: $p < .001$, Area ID: $p = .0315$, Elevation Zone: $p = .007$). A comparison of the

smooth terms showed that time was indeed a significant explanatory variable for the majority of nested observations, with only one smoothing function unable to explain the variance in the model (Area 3 Low Marsh: p = .2106). To test whether changing the model solved the issue of temporal heterogeneity, a variogram was constructed, using time as the "distance" variable. The output of this can be seen in Fig. 4.7. The resulting output indicates a mostly homogenous profile, which suggests that the violation of temporal independence has been addressed.

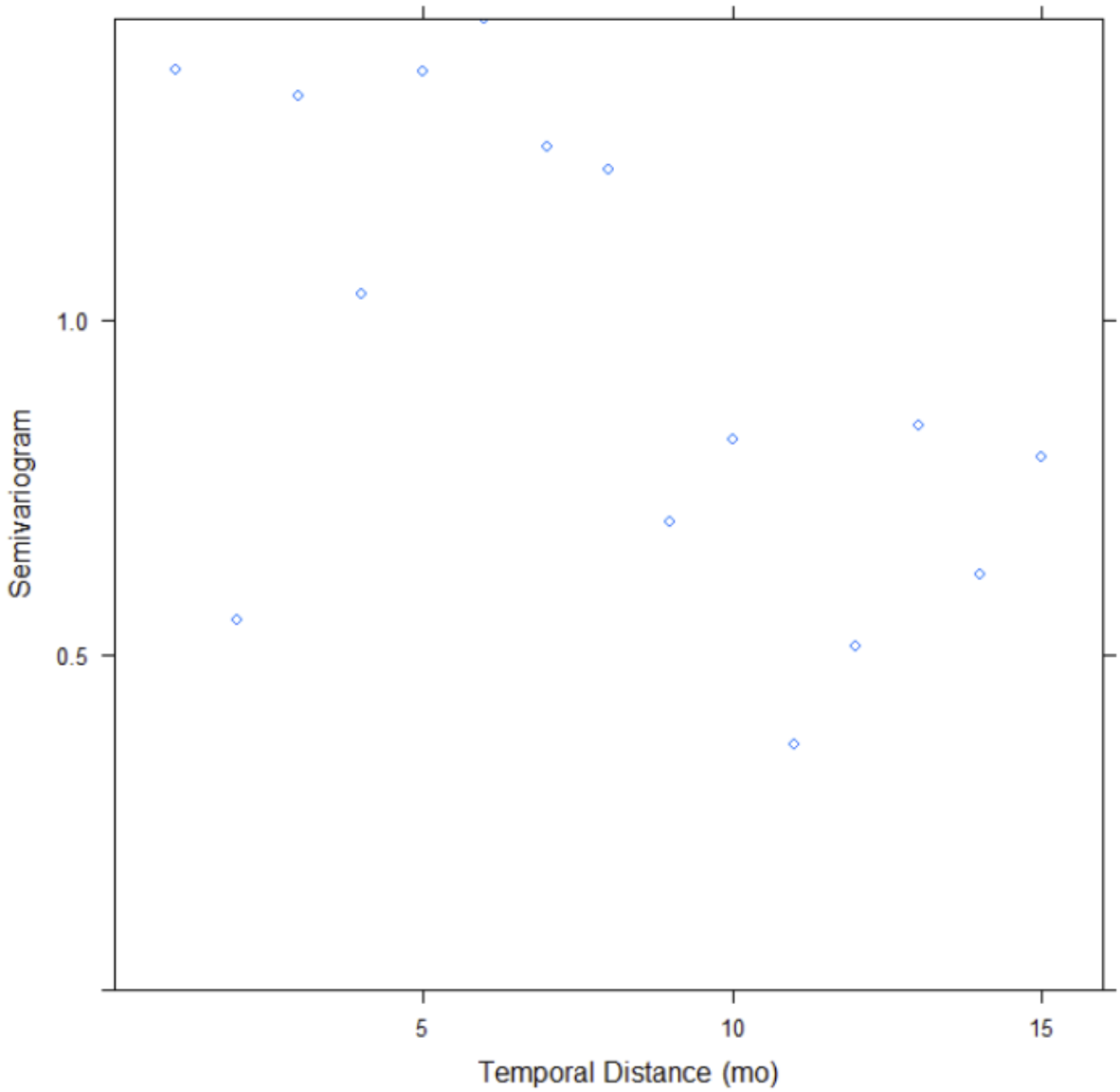

Figure 4.7: Variogram of improved temporal model using time as the distance variable. Homoscedasticity in the model will appear as the horizontal profile shown here.

CHAPTER 5

CONCLUSIONS

5.1 Initial Findings

The general pattern of NDVI improvement following the initial hurricane impact is similar to data from the Louisiana coastline following Hurricane Andrew (Courtemanche et. al, 1999), where it was found that percent cover tended to increase for plant communities within the marsh after the initial vegetation impact took place, although in this study the high marsh had more of this pronounced effect. Additionally, NDVI deviance seemed to increase for one additional month following the hurricane event before eventually improving, which was not observed in the Courtemanche study. While it took until mid-2018 for either elevation zone to see an increase in NDVI relative to that of a usual month, it is difficult to pinpoint when exactly either elevation zone returned to any sort of normalcy. The standard deviation from the median NDVI in the entire study was approximately .07, and if the standard deviation for the entire study is used as a threshold value, it would suggest that the low marsh zone ended up returning to an NDVI value that could be considered "normal" more rapidly than that of the high marsh zone by approximately three months. This lingering effect in the high marsh zone falls in line with predictions on how the different plant species in each elevation zone would react to hydrologic disturbance events (Shumway & Bertness, 1992).

What is unclear upon looking at these initial findings is to what extent the sudden drop in NDVI values in April of 2018 was caused by the hurricane, and to what extent external factors had on the sudden decrease in that month. While April 2018 does fall within the expected timeframe of continuing impact from the hurricane event as seen in similar studies, the sudden and steep decrease in NDVI breaks away from the slow, recovering trend that was seen in

previous months. Although this decrease could be caused by a delayed effect of the hurricane event, it is worth noting that April of 2018 was an unusually cold April for Galveston Island. Unfortunately, there are limited studies on the relationship between high marsh plant recovery and temperature, and while this sudden decrease does note the potential for temperature to play a factor in this vegetation recovery, the limited scope of this study makes further analysis of temperature as a potential variable difficult.

Baustian et al. (2015) also found plant recovery to spike in relation to sedimentation rates following Hurricane Katrina, although the current study had no accurate way of measuring the sedimentation rates from Harvey using remote sensing methods alone. Instead, it was found in this study that time and seasonality had a much more pronounced effect on the recovery of vegetation than environmental factors such as elevation zone, area ID, or slope, though these environmental factors had more effect on the initial impact following Harvey.

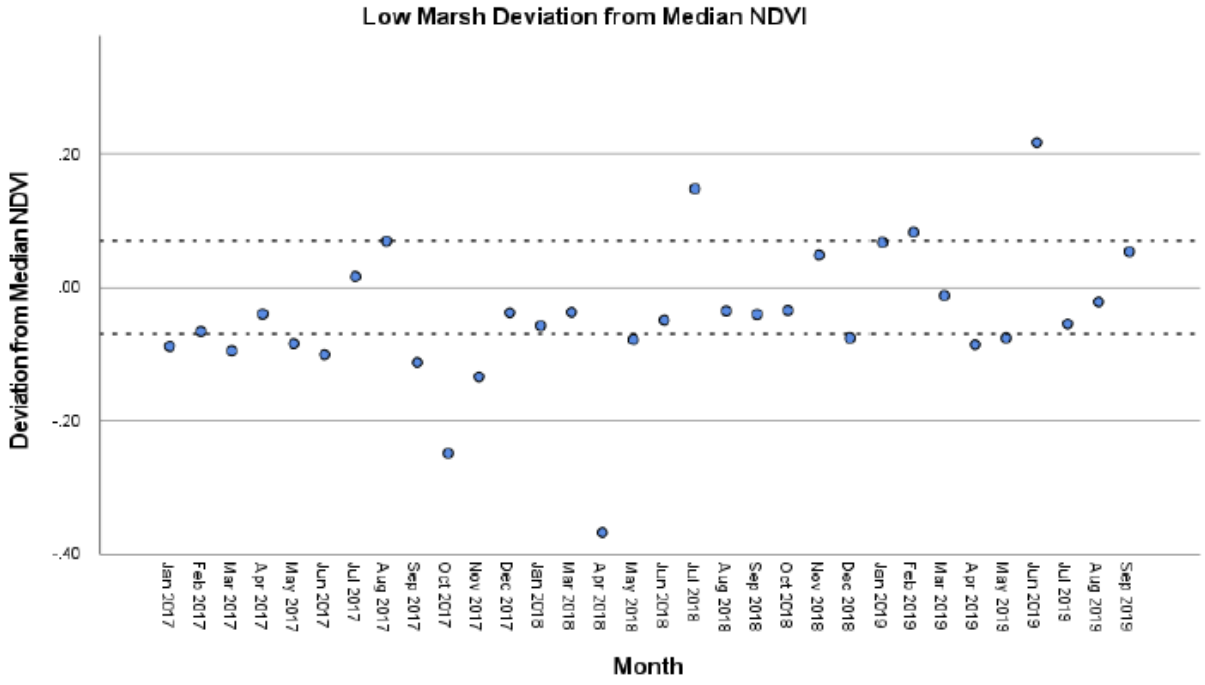

Figure 5.1: Time series of the deviation from the monthly median NDVI from January 2017 onwards for the low marsh zone. The horizontal bars represent one standard deviation away from the mean.

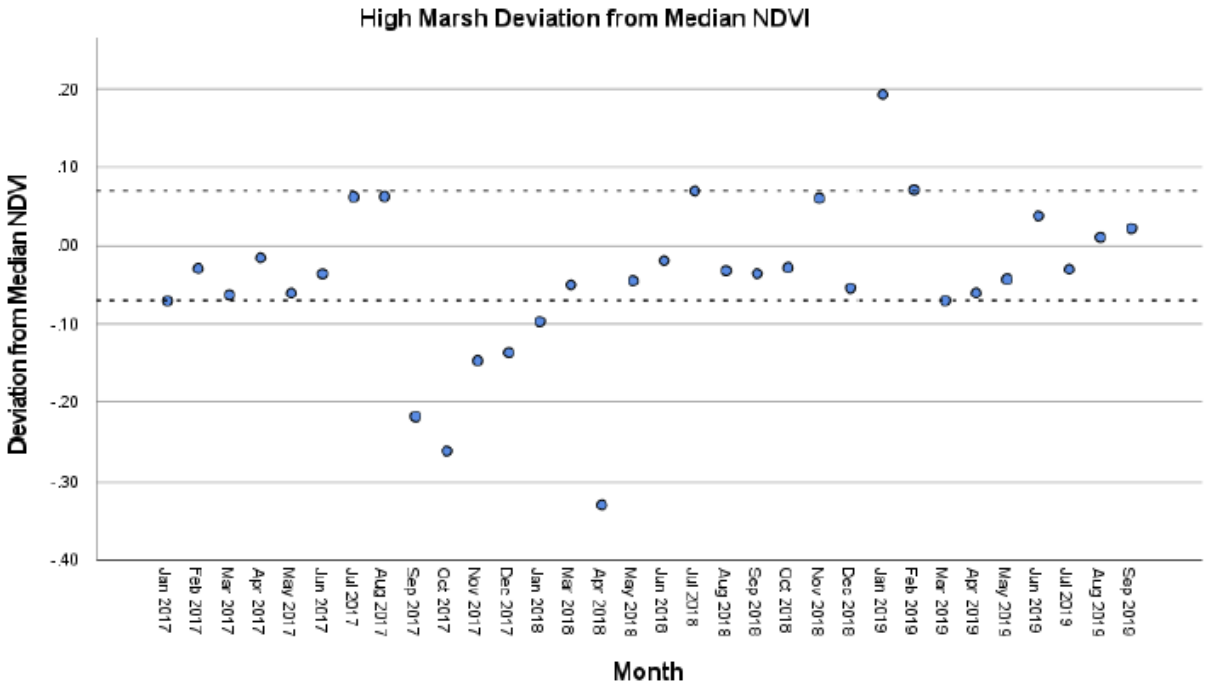

Figure 5.2: Time series of the deviation from the monthly median NDVI from January 2017 onwards for the high marsh zone. The horizontal bars represent one standard deviation away from the mean.

5.2 Slope

While slope initially seemed like a promising explanatory variable, the lack of any sort of statistical significance suggests that a closer look be taken at what slope in the context of this study actually does for the model and whether this role is ecologically significant or not. Salt marshes are generally characterized by wide, flat stretches of terrain with little vertical rise (Yapp, 1917). As salt marshes are defined by their elevation in relation to the tides, the upper extent of a salt marsh generally does not exceed 1-2m above sea level, whereas the horizontal stretch of a salt marsh extends for as long as the terrain allows. In this study, this horizontal extent can range from approximately 0.5 km in places like Area 3 to over 1 km wide in portions of Area 4. While this change in slope can look significant in that points of the marsh can quite literally have over double the slope as other points, the actual change in numeric value between

these points can be quite small regardless of the relationship between the slope of the two points. This becomes apparent when looking at a contour map similar to Fig 5.3 or a slope raster such as Fig 3.5.

This change in actual value of the slope becomes important when trying to predict what actual ecological impact that slope might have on this ecosystem after a hurricane. Slope was hypothesized to have an effect on the inundation times post-hurricane Harvey, which would then impact vegetative health and show a decrease in NDVI. However, this relationship between slope and inundation time could be broken if the actual change in slope is small. Essentially, if all the points in this study are similarly flat, then the numerical difference in "flatness" doesn't necessarily matter as much in regards to the difference in inundation times.

Where slope becomes interesting is in the context of intra-area variability. A look at the slope raster coupled with the available area of salt marsh that is in this study reveals that Areas 3 and 1 are really the two areas in this study that have any sort of major variability in slope. Repeating the spatial model described earlier in this thesis using only the points gathered from a single area resulted in increased statistical significance ($p = .057$ and .086 for Areas 3 and 1 respectively) for slope as an explanatory variable. While not meeting the 95% threshold for statistical significance, the fact that limiting the scope of the model to just a single area managed to increase the viability of slope to such a degree as a variable suggests that this variation in slope within a small, geographically similar area could still be ecologically important and at least partially explain variation within a smaller extent. This pattern seems to continue when looking at the individual points as well. When overlayed with the contour map in Figure 5.3, the steeper slopes along the margins of the small barrier islands in Area 3 as well as among the steeper regions of Area 1 show a decreased change in NDVI in corresponding data points relative to that

of their spatial neighbors with more gradual slopes. While there are other regions of steeper slopes in the slope rasters and in figure 5.3 along human-made structures and along the northwest region of the study area, these areas are difficult to draw conclusions from in the context of slope, as either there are no data points corresponding with these areas (in regards to human settlements, as these areas were excluded from the study due to not containing vegetation), or the data points therein also experience a shift in elevation zone from low marsh to high marsh (in regards to the northwest regions of the study area), making the actual link to slope as a variable difficult to determine due to the difference in plant species found along those points.

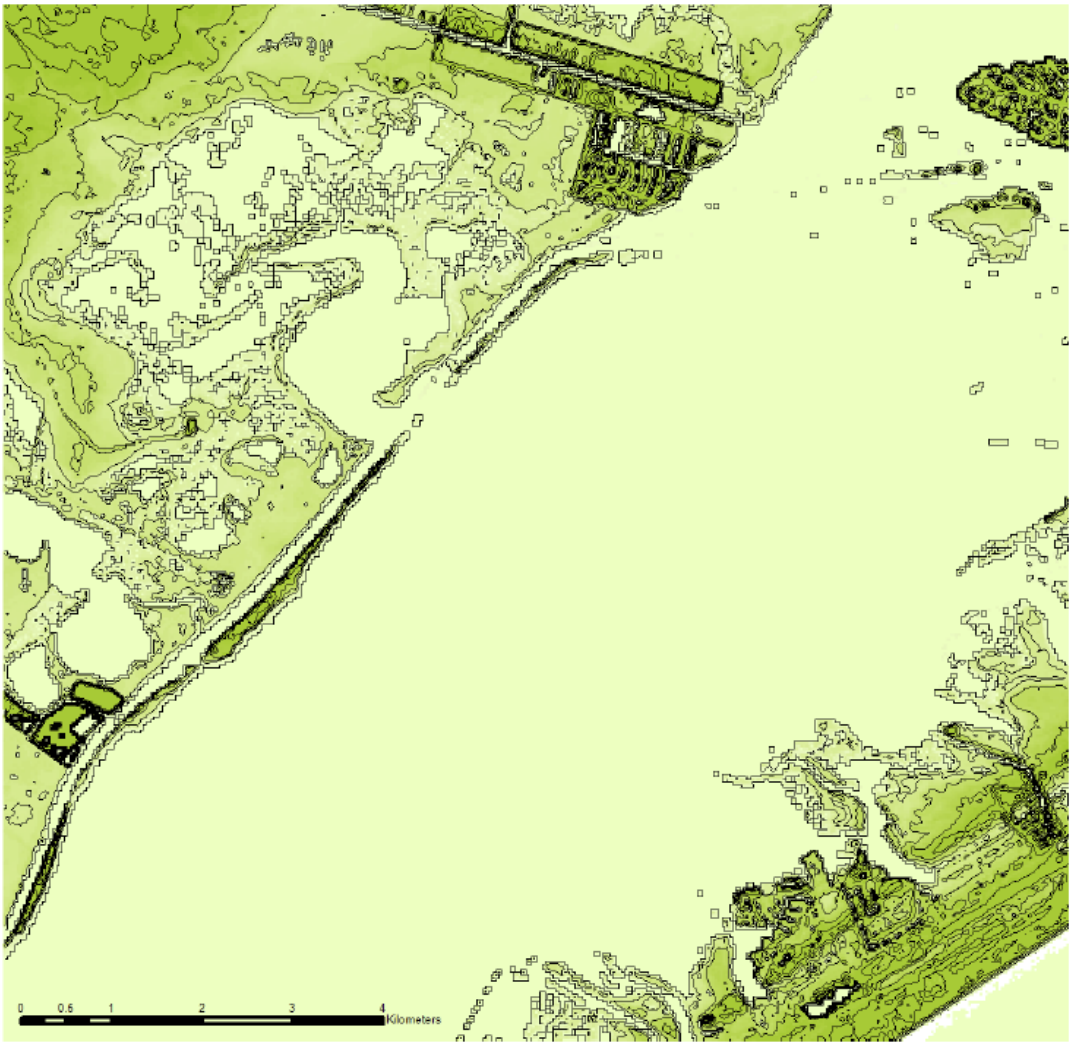

Figure 5.3: Contour map of the study area as generated from the LiDAR DTM. Each contour line represents half a meter of elevation rise.

5.3 Area 3

Area 3 remains quite distinct from the other geographic areas of the marsh in regards to both the initial change in NDVI as well as its response over time. While Area 3 didn't show an incredible deviation from other areas in regards to overall initial change, the variation within that initial change within Area 3 was much greater than any other geographic area of the marsh, and the temporal variation was such that the model discussed in the previous section was unable to fit an accurate smoother for the low marsh of this area. While this could be the cause of a missing covariate, it should also be worth noting that Area 3 is the area least insulated from storm surge given its position relative to that of Galveston Bay. Guntenspergen et al. (1995) established the importance of sediment load when discussing hurricane recovery in a Louisiana coastal marsh and, due to the topography of Area 3, it would suggest that this area in particular received a higher sediment load along the bay-facing edge compared to that of the other geographic areas. This higher sediment load along half of the area could explain the high variation of the area to the initial storm impact and the increased variation over time compared to that of other areas, although to test such a hypothesis would require further study. As hurricane storm surges are known to carry large quantities of sediment, this could be further evidence for the necessity of sedimentation rates as an additional explanatory variable (Williams, 2012).

Additionally, across all geographic areas, the low marsh zone suffered lessened initial impacts comparatively. This lessened impact could potentially be attributed to the specific species composition of intertidal marshes in the Texas Gulf Coast region. Mendelssohn and Morris (2002) note that the usually high productivity of *Spartina alterniflora*, the dominant species of Texas intertidal marshes, is highly dependent on abiotic factors such as soil anoxia and nitrates that are disrupted during sedimentation. This disruption in regards to the primary

production of the dominant species in these intertidal marshes could potentially explain some of the variability seen among low marsh zones in the model.

5.4 Ecological Implications

As with any ecological study containing categorical variables such as this one, it is important to understand what these categorical variables mean in an ecological sense. While it's easy enough to see from the results that a variable such as elevation zone was statistically significant in determining the impacts to NDVI following Hurricane Harvey, it's equally important to recognize that using elevation zone in this context is a way to geographically delineate the species zonation that is commonly seen in coastal salt marshes. Likewise, it's hardly enough to simply say that this species zonation had an effect on the initial and continuing impacts of Hurricane Harvey, but rather that the combined plant species that make up this zonation reacted differently to the impacts of hurricane Harvey, in such a way as to affect the overall biomass of a given point (Which is what NDVI in this study attempted to estimate). Thus, when the results revealed that the high marsh zone across all areas suffered a greater degree of initial NDVI loss, as well as a more prolonged recovery time compared to the low marsh zone, it could be argued that a more apt description of these results would be that the plant species that make up the high marsh zone were more adversely affected by this specific disturbance event, and took longer to recover from this disturbance than the more resilient species that are found in the low marsh.

This interpretation falls in line with other, similar research on the tolerances of high marsh plant species (Janousek & Mayo 2013), and could be considered applicable with the specific species assemblage of Galveston Island and West Bay. The plant species that commonly make up this part of the marsh include a mix of *Batis maritima*, *Salicornia virginica*, *Borrichia*

frutescens, *Juncus romerianus*, *Salicornia bigelovii*, *Monanthocloe littoralis*, *Suaeda linearis*, *Aster tenuifollus*, *Spartina patens*, and *Spartina spartinae*, although the last two are more commonly found in brackish marshes. While the individual salt and flooding tolerances of these species can vary (*Batis maritima*, *Salicornia virginica*, and *Juncus romerianus* are a bit more salt tolerant than the others on this list, and can sometimes be found along the higher elevations of the low marsh), the flooding and salt tolerances of all of these species pale in comparison to the dominant plant species that is found to inhabit the low marsh of this area: *Spartina alterniflora*. Given the natural resilience of *Spartina alterniflora* to the specific nature of disturbance that Harvey caused, coupled with the ability of *Spartina alterniflora* to rapidly recover and colonize disturbed patches of land (Coutemanche et al. 1999), the results of this lessened impact and rapid recovery in the low marsh was unsurprising.

Area ID, in the context of this study, was used primarily as a way to distinguish between portions of the study area that were predicted to receive different levels of storm surge, as storm surge would be impossible to quantify from satellite imagery and LiDAR alone. We know from hurricane reports after the fact which direction the wind and storm surge were traveling during the hurricane, and from that, the area ID categories were created based on the predicted level of impacts to this storm surge. With this in mind, the result of Area 2 suffering the least initial impact was surprising. Geographically, Area 2 contains many similar features as Area 4, but without the added benefit of a small barrier of addition marshland (Area 3) protecting it from storm surge. As the specific species composition of these areas doesn't drastically change from area-to-area, this would suggest that the reasoning for this decreased initial impact is physical in nature, although precisely what that reasoning might be is still unclear.

5.5 A Review of the Research Objectives

At the start of this research, we posed two main questions that this study attempted to answer. Firstly, which portions of the study area suffered the most vegetation damage due to Hurricane Harvey, and which environmental factors contributed the most to this damage? Secondly, is there a difference in recovery among these different portions in the months following Hurricane Harvey?

Following a review of the data, it seems clear that both elevation zone and area ID had a significant effect on the initial vegetation impacts of the hurricane, although slope, which was previously thought to be significant, did not turn out to be as significant as hypothesized. Specifically regarding which portions of the marshland suffered the most vegetation damage, it seems clear that the high marsh zone in particular suffered a greater degree of damage across all marsh areas. Among the marsh areas, Area 2 in particular suffered the least initial damage. While slope did not appear initially significant in regards to determining the initial vegetation impact, it did prove useful in explaining some of the variation within the specified marsh areas, although the extent of this relationship was unable to be determined in this study.

In regards to vegetation recovery, there did appear to be a difference in recovery among differing areas of the marsh. Area ID and elevation zone both proved significant in determining the vegetation response, though this significance seemed to decrease with time in favor of seasonality from a purely statistical standpoint. As far as elevation zones are concerned, the low marsh zone appeared to return to a state of "normal" more quickly than the high marsh zone. This would suggest that the specific characteristics of these elevation zones discussed previously in this thesis that lead the vegetation response in the short term, also help to drive the overall recovery of marsh vegetation in the long term.

5.6 Limitations of Environmental Modeling

Environmental modeling proved useful for this study in understanding the relationships between environmental factors and the impacts and recovery of vegetation following Hurricane Harvey. While the models in this study fit well for the data observed, it is unlikely that these same models could be useful in explaining the changes in future hurricanes or other such disturbance events. All the factors that made Harvey's impact on the Galveston coastline unique, such as species composition, geographic factors, and even specific attributes of the hurricane itself such as wind strength, flooding intensity, and storm surge could all vary wildly from hurricane to hurricane, and thus change how these environmental factors interact to influence vegetation growth and recovery.

While the model itself may not be applicable to other hurricanes and geographic regions, it is hypothesized that the significant factors that make up the model such as elevation zone, seasonality, and time could be similarly relevant in other studies. To what extent these variables could be relevant is uncertain, however it is encouraged that future, similar studies explore whether spatial variability in initial vegetation impacts is dependent on the variability of sedimentation rates after a large-scale storm event like Harvey.

APPENDIX

IMAGE SOURCES

Date Taken	Source	Cloud Cover	Processing Level
8/19/2005	Landsat 7	30%	LT1P
9/4/2005	Landsat 7	5%	LT1P
10/6/2005	Landsat 7	1%	LT1P
11/23/2005	Landsat 7	0%	LT1P
12/25/2005	Landsat 7	0%	LT1P
1/18/2006	Landsat 5	0%	LT1P
2/11/2006	Landsat 5	0%	LT1P
4/8/2006	Landsat 5	1%	LT1P
5/18/2006	Landsat 7	7%	LT1P
6/27/2006	Landsat 5	8%	LT1P
7/29/2006	Landsat 5	10%	LT1P
9/7/2006	Landsat 7	14%	LT1P
11/18/2006	Landsat 5	1%	LT1P
12/4/2006	Landsat 5	0%	LT1P
2/6/2007	Landsat 5	11%	LT1P
3/2/2007	Landsat 7	10%	LT1P
4/11/2007	Landsat 5	9%	LT1P
5/13/2007	Landsat 5	2%	LT1P
8/9/2007	Landsat 7	10%	LT1P
10/4/2007	Landsat 5	11%	LT1P
11/29/2007	Landsat 7	38%	LT1P
12/31/2007	Landsat 7	0%	LT1P
2/1/2008	Landsat 7	0%	LT1P
3/4/2008	Landsat 7	0%	LT1P
4/13/2008	Landsat 5	0%	LT1P
6/16/2008	Landsat 5	14%	LT1P
7/18/2008	Landsat 5	10%	LT1P
9/4/2008	Landsat 5	4%	LT1P
10/30/2008	Landsat 7	3%	LT1P
11/15/2008	Landsat 7	0%	LT1P
1/18/2009	Landsat 7	4%	LT1P

(table continues)

Date Taken	Source	Cloud Cover	Processing Level
2/3/2009	Landsat 7	0%	LT1P
4/8/2009	Landsat 7	4%	LT1P
5/18/2009	Landsat 5	8%	LT1P
7/13/2009	Landsat 7	9%	LT1P
8/22/2009	Landsat 5	4%	LT1P
9/7/2009	Landsat 5	23%	LT1P
10/17/2009	Landsat 7	0%	LT1P
11/2/2009	Landsat 7	2%	LT1P
12/20/2009	Landsat 7	0%	LT1P
1/21/2010	Landsat 7	44%	LT1P
2/6/2010	Landsat 7	0%	LT1P
3/18/2010	Landsat 5	0%	LT1P
5/5/2010	Landsat 5	0%	LT1P
6/14/2010	Landsat 7	13%	LT1P
8/1/2010	Landsat 7	2%	LT1P
10/4/2010	Landsat 7	3%	LT1P
11/5/2010	Landsat 7	0%	LT1P
12/15/2010	Landsat 7	30%	LT1P
1/8/2011	Landsat 7	13%	LT1P
2/25/2011	Landsat 7	10%	LT1P
3/21/2011	Landsat 5	16%	LT1P
5/16/2011	Landsat 7	11%	LT1P
6/1/2011	Landsat 7	8%	LT1P
7/3/2011	Landsat 7	10%	LT1P
8/28/2011	Landsat 5	0%	LT1P
9/5/2011	Landsat 7	3%	LT1P
10/15/2011	Landsat 5	4%	LT1P
11/24/2011	Landsat 7	36%	LT1P
1/11/2012	Landsat 7	0%	LT1P
5/18/2012	Landsat 7	12%	LT1P
7/5/2012	Landsat 7	20%	LT1P

(table continues)

Date Taken	Source	Cloud Cover	Processing Level
8/22/2012	Landsat 7	44%	LT1P
9/23/2012	Landsat 7	9%	LT1P
10/25/2012	Landsat 7	10%	LT1P
12/12/2012	Landsat 7	0%	LT1P
2/14/2013	Landsat 7	0%	LT1P
3/2/2013	Landsat 7	0%	LT1P
5/5/2013	Landsat 7	0%	LT1P
6/22/2013	Landsat 7	48%	LT1P
8/17/2013	Landsat 8	1%	LT1P
9/26/2013	Landsat 7	18%	LT1P
11/13/2013	Landsat 7	34%	LT1P
12/15/2013	Landsat 7	2%	LT1P
1/16/2014	Landsat 7	0%	LT1P
3/13/2014	Landsat 8	2%	LT1P
5/16/2014	Landsat 8	0%	LT1P
6/1/2014	Landsat 8	32%	LT1P
7/3/2014	Landsat 8	17%	LT1P
9/21/2014	Landsat 8	7%	LT1P
10/15/2014	Landsat 7	0%	LT1P
11/24/2014	Landsat 8	10%	LT1P
1/19/2015	Landsat 7	17%	LT1P
2/12/2015	Landsat 8	3%	LT1P
3/24/2015	Landsat 7	10%	LT1P
5/3/2015	Landsat 8	19%	LT1P
6/4/2015	Landsat 8	24%	LT1P
7/22/2015	Landsat 8	11%	LT1P
8/23/2015	Landsat 8	9%	LT1P
9/8/2015	Landsat 8	13%	LT1P
10/18/2015	Landsat 7	9%	LT1P
11/19/2015	Landsat 7	0%	LT1P
12/5/2015	Landsat 7	10%	LT1P

(table continues)

Date Taken	Source	Cloud Cover	Processing Level
1/22/2016	Landsat 7	26%	LT1P
2/7/2016	Landsat 7	0%	LT1P
3/2/2016	Landsat 8	18%	LT1P
4/27/2016	Landsat 7	28%	LT1P
5/13/2016	Landsat 7	12%	LT1P
6/6/2016	Landsat 8	19%	LT1P
7/16/2016	Landsat 7	14%	LT1P
8/1/2016	Landsat 7	6%	LT1P
9/2/2016	Landsat 7	18%	LT1P
10/28/2016	Landsat 8	4%	LT1P
11/5/2016	Landsat 7	19%	LT1P
12/25/2016	Sentinel-2	3%	1C
1/24/2017	Landsat 7	1%	LT1P
2/1/2017	Landsat 8	19%	LT1P
3/21/2017	Landsat 8	0%	LT1P
4/6/2017	Landsat 8	0%	LT1P
5/24/2017	Landsat 8	0%	LT1P
6/9/2017	Landsat 8	34%	LT1P
7/3/2017	Landsat 7	15%	LT1P
8/20/2017	Landsat 7	9%	LT1P
9/11/2017	Sentinel-2	0%	1C
10/11/2017	Sentinel-2	0%	1C
11/15/2017	Sentinel-2	1%	1C
12/10/2017	Landsat 7	9%	LT1P
1/3/2018	Landsat 8	19%	LT1P
3/30/2018	Sentinel-2	0%	1C
4/17/2018	Landsat 7	0%	LT1P
5/27/2018	Landsat 8	11%	LT1P
6/28/2018	Landsat 8	19%	LT1P
7/23/2018	Sentinel-2	13%	1C
8/7/2018	Landsat 7	20%	LT1P

(table continues)

Date Taken	Source	Cloud Cover	Processing Level
9/24/2018	Landsat 7	19%	LT1P
10/26/2018	Landsat 7	10%	LT1P
11/15/2018	Sentinel-2	0%	1C
12/21/2018	Landsat 8	0%	LT1P
1/6/2019	Landsat 8	10%	LT1P
2/13/2019	Sentinel-2	0%	1C
3/27/2019	Landsat 8	4%	LT1P
4/20/2019	Landsat 7	0%	LT1P
5/14/2019	Landsat 8	29%	LT1P
6/8/2019	Sentinel-2	1%	1C
7/9/2019	Landsat 7	9%	LT1P
8/18/2019	Landsat 8	24%	LT1P

REFERENCES

Bartlett, D. S., & Klemas, V. (1980). Quantitative assessment of emergent Spartina alterniflora biomass in tidal wetlands using remote sensing. In *Estuarine and Wetland Processes* (pp. 425-436). Springer, Boston, MA.

Baumann, R. H., Day, J. W., & Miller, C. A. (1984). Mississippi deltaic wetland survival: sedimentation versus coastal submergence. *Science*, *224*(4653), 1093-1095.

Baustian, J. J., & Mendelssohn, I. A. (2015). Hurricane-induced sedimentation improves marsh resilience and vegetation vigor under high rates of relative sea level rise. *Wetlands*, *35*(4), 795-802.

Bertness, M. D., & Ellison, A. M. (1987). Determinants of pattern in a New England salt marsh plant community. *Ecological Monographs*, *57*(2), 129-147.

Best, Ü. S., Van der Wegen, M., Dijkstra, J., Willemsen, P. W. J. M., Borsje, B. W., & Roelvink, D. J. (2018). Do salt marshes survive sea level rise? Modelling wave action, morphodynamics and vegetation dynamics. *Environmental modelling & software*, *109*, 152-166.

Bird, E. C. F., & Ranwell, D. S. (1964). Spartina salt marshes in Southern England: IV. the physiography of Poole Harbour, Dorset. *The Journal of Ecology*, 355-366.

Blake, E. S., & Zelinsky, D. A. (2018). *National Hurricane Center Tropical Cyclone Report: Hurricane Harvey (17 August - 1 September 2017)*. United States. National Oceanic and Atmospheric Administration.

Brown, C. W. (1939). Hurricanes and shore-line changes in Rhode Island. *Geographical Review*, *29*(3), 416-430.

Cahoon, D. R., & Reed, D. J. (1995). Relationships among marsh surface topography, hydroperiod, and soil accretion in a deteriorating Louisiana salt marsh. *Journal of Coastal Research*, 357-369.

Chapman, V. J. (1974). Salt marshes and salt deserts of the world. *Ecology of halophytes*, 3-19.

Colwell, R. (1956). Determining the prevalence of certain cereal crop diseases by means of aerial photography. *Hilgardia*, *26*(5), 223-286.

Conard, H. S., & Galligar, G. C. (1929). Third survey of a Long Island salt marsh. *Ecology*, *10*(3), 326-336.

Conner, W. H., Day, J. W., Baumann, R. H., & Randall, J. M. (1989). Influence of hurricanes on coastal ecosystems along the northern Gulf of Mexico. *Wetlands Ecology and Management*, *1*(1), 45–56. doi: 10.1007/bf00177889

Cooper, A. (1982). The effects of salinity and waterlogging on the growth and cation uptake of salt marsh plants. *New phytologist*, *90*(2), 263-275.

Courtemanche Jr, R. P., Hester, M. W., & Mendelssohn, I. A. (1999). Recovery of a Louisiana barrier island marsh plant community following extensive hurricane-induced overwash. *Journal of Coastal Research*, 872-883.

Dangwal, N. (2014). Detection of crop water stress and its impact on productivity of cropland ecosystem. *India: Jurnal Andhra University*.

Davenport, I. J., Mason, D. C., Robinson, G. J., Flatbed, R. A., Amin, M., Smith, J. A., & Gurney, C. (1970). A digital elevation model of sections of the UK intertidal zone from the integration of satellite imagery and ocean height modelling. *WIT Transactions on Ecology and the Environment*, *25*.

Engels, J. G., & Jensen, K. (2009). Patterns of wetland plant diversity along estuarine stress gradients of the Elbe (Germany) and Connecticut (USA) Rivers. *Plant Ecology & Diversity*, *2*(3), 301-311.

Ewanchuk, P. J., & Bertness, M. D. (2003). Recovery of a northern New England salt marsh plant community from winter icing. *Oecologia*, *136*(4), 616–626. doi: 10.1007/s00442-003-1303-7

Gedan, K. B., & Bertness, M. D. (2010). How will warming affect the salt marsh foundation species Spartina patens and its ecological role? *Oecologia*, *164*(2), 479–487. doi: 10.1007/s00442-010-1661-x

Griggs, R. F. (1918). The Recovery of Vegetation at Kodiak (Part I in Series).

Guntenspergen, G. R., Cahoon, D. R., Grace, J., Steyer, G. D., Fournet, S., Townson, M. A., & Foote, A. L. (1995). Disturbance and recovery of the Louisiana coastal marsh landscape from the impacts of Hurricane Andrew. *Journal of Coastal Research*, 324-339.

Harshberger, J. W. (1916). The origin and vegetation of salt marsh pools. *Proceedings of the American Philosophical Society*, *55*(6), 481-484

Howard, R. A. (1950). Vegetation of the Bimini Island Group: Bahamas, BWI. *Ecological Monographs*, *20*(4), 317-349.

Huang, C., Peng, Y., Lang, M., Yeo, I. Y., & McCarty, G. (2014). Wetland inundation mapping and change monitoring using Landsat and airborne LiDAR data. *Remote Sensing of Environment*, *141*, 231-242.

Huckle, J. M., Potter, J. A., & Marrs, R. H. (2000). Influence of environmental factors on the growth and interactions between salt marsh plants: effects of salinity, sediment and waterlogging. *Journal of Ecology*, *88*(3), 492-505.

Janousek, C.N., Mayo, C. Plant responses to increased inundation and salt exposure: interactive effects on tidal marsh productivity. *Plant Ecol* **214,** 917–928 (2013). https://doi.org/10.1007/s11258-013-0218-6

Kindle, E. M. (1937). Post hurricane sea shore observations. *American Midland Naturalist*, *18*(3), 426-434.

King, S. E., & Lester, J. N. (1995). The value of salt marsh as a sea defence. *Marine Pollution Bulletin*, *30*(3), 180–189. doi: 10.1016/0025-326x(94)00173-7

Kinyanjui, M. J. (2011). NDVI-based vegetation monitoring in Mau forest complex, Kenya. *African Journal of Ecology*, *49*(2), 165-174.

Kunza, A. E., & Pennings, S. C. (2008). Patterns of Plant Diversity in Georgia and Texas Salt Marshes. *Estuaries and Coasts*, *31*(4), 673–681. doi: 10.1007/s12237-008-9058-3

Langbein, W. B. (1947). Topographic characteristics of drainage basins.

Lyu, H. M., Wang, G. F., Shen, J. S., Lu, L. H., & Wang, G. Q. (2016). Analysis and GIS mapping of flooding hazards on 10 May 2016, Guangzhou, China. *Water*, *8*(10), 447.

Mendelssohn, I. A., & Morris, J. T. (2002). Eco-physiological controls on the productivity of Spartina alterniflora Loisel. *Concepts and controversies in tidal marsh ecology*, 59-80.

New York City Panel on Climate Change. (2013). Climate risk information 2013: observations, climate change projections, and maps. *NPCC2. Available at http://www. nyc. gov/html/planyc2030/downloads/pdf/npcc_climate_risk_information_2013_report. pdf. Published June*, *11*.

Nowell, W. R., & Parrish, D. W. (1956). Effectiveness of a pre-hatching Treatment for the Control of Salt-marsh Mosquitoes in Florida. *Mosquito News*, *16*(3).

Parker, J. A., Kenyon, R. V., & Troxel, D. E. (1983). Comparison of interpolating methods for image resampling. *IEEE Transactions on medical imaging*, *2*(1), 31-39.

Pennings, S. C., Grant, M.-B., & Bertness, M. D. (2005). Plant zonation in low-latitude salt marshes: disentangling the roles of flooding, salinity and competition. *Journal of Ecology*, *93*(1), 159–167. doi: 10.1111/j.1365-2745.2004.00959.x

Portnoy, J. W., & Valiela, I. (1997). Short-term effects of salinity reduction and drainage on salt-marsh biogeochemical cycling andSpartina (cordgrass production. *Estuaries*, *20*(3), 569-578.

Quintana, X. D., Comiín, F. A., & Moreno-Amich, R. (1998). Nutrient and plankton dynamics in a Mediterranean salt marsh dominated by incidents of flooding. Part 2: Response of the zooplankton community to disturbances. *Journal of Plankton Research*, *20*(11), 2109–2127. doi: 10.1093/plankt/20.11.2109

Reed, D. J., & Cahoon, D. R. (1992). The relationship between marsh surface topography, hydroperiod, and growth of Spartina alterniflora in a deteriorating Louisiana salt marsh. *Journal of Coastal Research*, 77-87.

Reidenbaugh, T. G., & Banta, W. C. (1980). Origins and Effects of Spartina Wrack in a Virginia Salt Marsh. *Gulf Research Reports*, *6*. doi: 10.18785/grr.0604.07

Rodgers, J. C., Murrah, A. W., & Cooke, W. H. (2009). The Impact of Hurricane Katrina on the Coastal Vegetation of the Weeks Bay Reserve, Alabama from NDVI Data. *Estuaries and Coasts*, *32*(3), 496–507. doi: 10.1007/s12237-009-9138-z

Roman, C. T., Niering, W. A., & Warren, R. S. (1984). Salt marsh vegetation change in response to tidal restriction. *Environmental Management*, *8*(2), 141-149.

Rouse, J. W., Haas, R. H., Schell, J. A., Deering, D. W., & Harlan, J. C. (1974). Monitoring the vernal advancement and retrogradation (green wave effect) of natural vegetation. *NASA/GSFC Type III Final Report, Greenbelt, Md*, *371*.

Sebastian, A., Gori, A., Blessing, R. B., van der Wiel, K., & Bass, B. (2019). Disentangling the impacts of human and environmental change on catchment response during Hurricane Harvey. *Environmental Research Letters*, *14*(12), 124023.

Schrift, A. M., Mendelssohn, I. A., & Materne, M. D. (2008). Salt marsh restoration with sediment-slurry amendments following a drought-induced large-scale disturbance. *Wetlands*, *28*(4), 1071–1085. doi: 10.1672/07-78.1

Shaler, N. S. (1885). *Preliminary report on sea-coast swamps of the eastern United States*. US Geological survey.

Shumway, S. W., & Bertness, M. D. (1992). Salt stress limitation of seedling recruitment in a salt marsh plant community. *Oecologia*, *92*(4), 490-497.

Steyer, G. D., Couvillion, B. R., & Barras, J. A. (2013). Monitoring Vegetation Response to Episodic Disturbance Events by using Multitemporal Vegetation Indices. *Journal of Coastal Research*, *63*, 118–130. doi: 10.2112/si63-011.1

Touchette, B. W., Kneppers, M. K., & Eggert, C. M. (2019). Salt marsh plants: biological overview and vulnerability to climate change. *Halophytes and Climate Change: Adaptive Mechanisms and Potential Uses*, 115–134. doi: 10.1079/9781786394330.0115

Tucker, C. J. (1977). Use of near infrared/red radiance ratios for estimating vegetation biomass and physiological status.

Vogelmann, J. E., Howard, S. M., Yang, L., Larson, C. R., Wylie, B. K., & Van Driel, N. (2001). Completion of the 1990s National Land Cover Data Set for the conterminous United States from Landsat Thematic Mapper data and ancillary data sources. *Photogrammetric Engineering and Remote Sensing*, *67*(6).

Wang, C., Menenti, M., Stoll, M. P., Feola, A., Belluco, E., & Marani, M. (2009). Separation of ground and low vegetation signatures in LiDAR measurements of salt-marsh environments. *IEEE Transactions on Geoscience and Remote Sensing*, *47*(7), 2014-2023.

Weier, J., & Herring, D. (2000). Measuring vegetation (ndvi & evi). *NASA Earth Observatory*, *20*.

Williams, H. F. (2012). Magnitude of Hurricane Ike storm surge sedimentation: implications for coastal marsh aggradation. *Earth Surface Processes and Landforms*, *37*(8), 901-906.

Yapp, R. H., Johns, D., & Jones, O. T. (1917). The salt marshes of the Dovey Estuary. *The Journal of Ecology*, 65-103.

Zedler, J. B., Covin, J., Nordby, C., Williams, P., & Boland, J. (1986). Catastrophic Events Reveal the Dynamic Nature of Salt-Marsh Vegetation in Southern California. *Estuaries*, *9*(1), 75. doi: 10.2307/1352195

Zhang, C. (2020). Assessing the Effects of Hurricane Irma on Mangrove Structures in the Coastal Everglades using Airborne Lidar Data. *Multi-sensor System Applications in the Everglades Ecosystem*, 289.

Zhang, M., Ustin, S. L., Rejmankova, E., & Sanderson, E. W. (1997). Monitoring Pacific coast salt marshes using remote sensing. *Ecological Applications*, *7*(3), 1039-1053.

Zhou, X., Armitage, A. R., & Prasad, S., "Mapping mangrove communities in coastal wetlands using airborne hyperspectral data," *2016 8th Workshop on Hyperspectral Image and Signal Processing: Evolution in Remote Sensing (WHISPERS)*, Los Angeles, CA, 2016, pp. 1-5.